AWARD NUMBER: W81XWH-17-1-0653

TITLE: Temporal Evolution of N-Myc Signaling and Early Targeting of the Neuroendocrine Phenotype in Prostate Cancer

PRINCIPAL INVESTIGATOR: Himisha Beltran

CONTRACTING ORGANIZATION: Dana-Farber Cancer institute, Boston, MA

REPORT DATE: October 2022

TYPE OF REPORT: Annual

PREPARED FOR: U.S. Army Medical Research and Development Command
Fort Detrick, Maryland 21702-5012

REPORT DOCUMENTATION PAGE

Form Approved
OMB No. 0704-0188

1. REPORT DATE	2. REPORT TYPE	3. DATES COVERED
October 2022	Annual	30Sep2021-29Sep2022

4. TITLE AND SUBTITLE

Temporal Evolution of N-Myc Signaling and Early Targeting of the Neuroendocrine Phenotype in Prostate Cancer

5a. CONTRACT NUMBER

5b. GRANT NUMBER
W81XWH-17-1-0653

5c. PROGRAM ELEMENT NUMBER

6. AUTHOR(S)

Himisha Beltran

E-Mail: himisha_beltran@dfci.harvard.edu

5d. PROJECT NUMBER

5e. TASK NUMBER

5f. WORK UNIT NUMBER

7. PERFORMING ORGANIZATION NAME(S) AND ADDRESS(ES)

DANA-FARBER CANCER INSTITUTE, INC.
BOSTON MA 02115-5418

8. PERFORMING ORGANIZATION REPORT NUMBER

9. SPONSORING / MONITORING AGENCY NAME(S) AND ADDRESS(ES)

U.S. Army Medical Research and Development Command
Fort Detrick, Maryland 21702-5012

10. SPONSOR/MONITOR'S ACRONYM(S)

11. SPONSOR/MONITOR'S REPORT NUMBER(S)

12. DISTRIBUTION / AVAILABILITY STATEMENT

Approved for Public Release; Distribution Unlimited

13. SUPPLEMENTARY NOTES

14. ABSTRACT

Transformation of castration resistant prostate cancer (CRPC) towards androgen signaling independence has emerged as a resistance mechanism in a subset of metastatic CRPC following exposure to androgen receptor (AR)-targeted therapies such as abiraterone or enzalutamide. Clinically, patients typically present with progression in the setting of a low or modestly rising serum prostate specific antigen (PSA) and metastatic biopsies can show pathologic or molecular features consistent with neuroendocrine prostate cancer (NEPC). NEPC is associated with low or absent AR expression, suppressed AR signaling, retention of early genomic mutations from its adenocarcinoma precursor, and acquisition of distinct genomic and epigenomic alterations (Beltran H, et al, Nature Medicine, 2016). The development of novel therapeutic approaches for patients with NEPC represents a clinical unmet need. Over the last seven years, our group has focused on characterizing the molecular landscape of NEPC and have identified and validated new therapeutic targets, including the N-Myc/Aurora A pathway and specific epigenetic modifiers such as (Enhancer of Zeste Homolog 2) EZH2 (Beltran H, Rickman DS et al Cancer Discovery 2011; Dardenne E, Beltran H, …. and Rickman DS, Cancer Cell 2016).

15. SUBJECT TERMS
None listed.

16. SECURITY CLASSIFICATION OF:			17. LIMITATION OF ABSTRACT	18. NUMBER OF PAGES	19a. NAME OF RESPONSIBLE PERSON
a. REPORT	b. ABSTRACT	c. THIS PAGE			USAMRDC
Unclassified	Unclassified	Unclassified	Unclassified	29	19b. TELEPHONE NUMBER *(include area code)*

TABLE OF CONTENTS

1. INTRODUCTION:

Lineage plasticity and histologic transformation of prostate cancer to a small cell neuroendocrine prostate cancer (NEPC) has emerged as a resistance mechanism in a subset of patients with metastatic prostate cancer following exposure to androgen receptor (AR)-targeted therapies. NEPC is associated with low or absent AR expression, suppressed AR signaling, retention of early genomic mutations from its adenocarcinoma precursor, and acquisition of distinct genomic and epigenomic alterations (Beltran H, et al, Nature Medicine, 2016). The development of novel therapeutic approaches for patients with NEPC represents a clinical unmet need. Over the last ten years, we have worked together to characterize the molecular landscape of NEPC and have identified and validated new therapeutic targets, including the N-Myc/Aurora A pathway and specific epigenetic modifiers such as (Enhancer of Zeste Homolog 2) EZH2 (Beltran H, Rickman DS et al Cancer Discovery 2011; Dardenne E, Beltran H, …. and Rickman DS, Cancer Cell 2016).

Hypothesis: N-Myc is an early driver of the NEPC phenotype, and that by tracking N-Myc signaling during the transition from adenocarcinoma to NEPC, we can identify cooperating factors that promote NEPC progression and define appropriate time points for early intervention.

To address this hypothesis, we formulated 3 Specific Aims:

Specific Aim 1: To assess the timing of N-Myc activation in patients and define how N-Myc and NEPC signaling impacts prognosis. The working hypothesis of this **Aim** is that there are specific molecular changes that serve as early markers of tumors that will evolve to NEPC. We will assess patient tumors at various timepoints during disease progression from prostate adenocarcinoma to NEPC and correlate N-Myc expression and NEPC signaling with clinical features and outcomes. We will also investigate MYCN and AURKA genomic amplification in tumors and circulating tumor DNA (ctDNA). Specifically, we will evaluate: 1) localized prostate cancer patients treated with prostatectomy; 2) high risk localized patients treated with or without neoadjuvant docetaxel and androgen deprivation therapy (NCT00430183); 3) patients with metastatic CRPC treated with abiraterone, and enzalutamide (IRB1305013903, PI Beltran); 4) NEPC patients treated with the Aurora A inhibitor MLN8237 (NCT01799278, PI Beltran). Gene expression will be quantified using a custom-designed assay validated by our group and amenable to FFPE tissues. N-Myc, Aurora A, and AR signaling genes, stem cell, neuronal, and other NEPC markers will be assessed. AURKA and MYCN amplification will be evaluated in tumors and ctDNA by targeted exome sequencing and/or FISH. We predict that N-Myc/NEPC signaling may be detected early in a subset of high-risk patients and this represents the presence of treatment resistant cells, and that this signaling program is enhanced after both short and long term AR-targeted therapies. The detection and determination of the frequency of early NEPC-associated alterations will help molecularly define subsets of prostate adenocarcinomas as harbingers of NEPC. This has clinical implications towards the development of diagnostic, prognostic, and predictive biomarkers to be evaluated early (potentially at the time of prostate cancer diagnosis) to select individuals at high risk for progression for early intervention. These results will also help identify patients less likely to benefit from AR-targeted strategies and more likely to benefit from MLN8237 or other N-Myc directed approaches.

Specific Aim 2: To assess the impact of timing of N-Myc expression on the development of castration resistance and the NEPC phenotype. The working hypothesis of this **Aim** is that N-Myc drives the trans-differentiation of castration resistant adenocarcinomas towards the NEPC phenotype. In order to model the evolutionary acquisition of N-Myc signaling during prostate cancer progression, we will temporally regulate N-Myc expression either at (3 months) or after (6 months and 9 months) the time of disease onset following Pten deletion both in intact mice and in mice castrated at 6 months. We will monitor Pten mutant cells (using YFP) before N-Myc and after N-Myc (Td-Tomato) overexpression and lineage trace emerging clones that develop histological and molecular features of NEPC. We expect that castration will lead to a quicker N-Myc-induced onset of NEPC.

Specific Aim 3: To evaluate the influence of N-Myc timing on response to NEPC directed therapeutics. The working hypothesis of this **Aim** is that N-Myc over-expression sensitizes CRPC to

NEPC-directed therapeutics. We will test N-Myc-early and N-Myc-late models with drugs that have demonstrated efficacy against NEPC including Aurora kinase A inhibition, platinum chemotherapy and EZH2 inhibitors. We will also evaluate the effect of the EZH2 inhibitors as priming agents with Aurora-A or AR-directed therapies (enzalutamide) in delaying or reversing AR-independent resistance *in vitro* and *in vivo*. We predict that early N-Myc expression results in comparable response to N-Myc targeted therapies as NEPC and early treatment with these agents modulates NEPC transcriptional programs. Results from this **Aim** will aid in biomarker selection for future trials.

2. KEYWORDS:

Castration resistant prostate cancer (CRPC), androgen receptor (AR)-targeted therapy, neuroendocrine prostate cancer (NEPC), N-Myc transcription factor (N-Myc), Polycomb Repressive Complex 2-associated protein Enhancer of Zeste Homolog 2 (EZH2).

3. ACCOMPLISHMENTS:

What were the major goals of the project?

1. Specific Aim 1: To assess the timing of N-Myc activation in patients and define how N-Myc signaling impacts response to aurora kinase A inhibition and clinical outcomes.
    a. Evaluate localized prostate cancer patients treated with prostatectomy
    b. Evaluate high risk localized patients treated with or without neoadjuvant docetaxel and androgen deprivation therapy (NCT00430183).
    c. Evaluate pre-treatment metastatic biopsies from CRPC patients treated with abiraterone, and enzalutamide (IRB1305013903).
    d. Evaluate pre-treatment metastatic biopsies from NEPC patients treated with the Aurora A inhibitor MLN8237 (NCT01799278) on a Phase 2 clinical trial or the EZH2 inhibitor GSK126 (NCT02082977).

2. Specific Aim 2: Assess the impact of timing of N-Myc expression on the development of castration resistance and the NEPC phenotype.
    a. Assess the influence of N-Myc on the onset of CRPC and NEPC and associated molecular changes.
    b. Assess the role of N-Myc/EZH2 complex for N-Myc dependent transcriptional regulation in establishing the NEPC phenotype.
    c. Assess the role of N-Myc/Aurora-A complex for N-Myc dependent transcriptional regulation in establishing the NEPC phenotype

3. Specific Aim 3: Determine the impact of the timing of N-Myc on response to NEPC directed therapeutics.
    a. Monitor the impact of the timing of N-Myc expression in response to NEPC-related monotherapies *in vivo* and *in vitro.*
    b. Monitor the impact of the timing of N-Myc expression in response to NEPC-related combination therapies *in vivo* and *in vitro.*
    c. Mechanistic studies to determine NEPC-related molecular changes associated with EZH2 and Aurora A inhibition *in vitro* and *in vivo*

What was accomplished under these goals?

The last progress report for this Award was submitted in November 2022 with a NCE request. Additional updates are included here.

1. **Specific Aim 1: To assess the timing of N-Myc activation in patients and define how N-Myc signaling impacts response to aurora kinase A inhibition and clinical outcomes.**

CALGB 90203. We are evaluating DNA and RNA from prostatectomy samples from patients with high risk localized prostate cancer from patients on the Phase 3 CALGB 90203 trial and have made significant progress. The rationale relevant to this DOD Specific Aim 1 is to identify molecular features of lineages plasticity in tumors treated with short term systemic therapy (ADT plus docetaxel for 6 months). We assembled a correlative cohort of 471 radical prostatectomy tumor tissues with central pathology review from patients enrolled on CALGB 90203 (ALLIANCE) from 2006 to 2015. We performed targeted DNA sequencing and mRNA expression profiling on tumor foci and adjacent non-cancer regions and tested for associations with pathologic changes and clinical outcomes. Tumor fraction estimated from DNA sequencing was significantly lower in treated tissues compared to those from the surgery-only arm. Higher tumor fraction after therapy was associated with aggressive pathologic features and poor clinical outcomes including shorter PSA-PFS (univariate HR 6.30; 95% CI 1.85 - 21.49; $p < 0.005$). *SPOP* mutations were infrequently detected after chemohormonal therapy, while *TP53* mutations were enriched and associated with shorter overall survival. Residual tumor fraction post-treatment was linked with higher expression of AR-regulated, cell cycle-related, and neuroendocrine-related genes, collectively suggesting persistent populations of active prostate cancer cells. Supervised clustering using genes that were differentially expressed in post-treated high tumor fraction tissues identified a distinct group of patients with elevated cell cycle related gene expression and poor clinical outcomes. While N-myc was not significantly upregulated post-therapy in all patients, these data do suggest that lineage plasticity changes can occur in a subset of patients with high-risk prostate cancer after short term-ADT and chemotherapy.

Phase 2 trial of MLN8237. We are also evaluating N-myc status in pre-treatment biopsies from the MLN8237 treated cohort and transcriptome data was subsequently published (Beltran et al CCR 2019). Notably, we identified exceptional responder to MLN8237 with N-myc and Aurora co-amplification who was maintained on study drug for >3.5 years. We also developed a patient derived organoid from a non-responder patient (PM154) whose tumor had very high levels of N-myc-Aurora- A complex formation (as seen by proximal ligation assay). MLN8237 was not capable of disrupting the complex in vitro (vs. LnCap-n-myc control cells), and we are developing novel strategies using this PM154 organoid as well as a MLN8237 NEPC organoid PM155 that we developed as clinically relevant models to assess on-target activity.

Patients with biopsy confirmed CRPC/NEPC and those treated with AR pathway inhibitors. 76 patient biopsies were grouped according to their tumor histological classification (CRPC or NEPC) and stratified into three categories based on RNA-seq values of *MYCN* expression (high vs. low) and *RB1* genomic status (deletion, yes vs. no). Of the 76 patient samples, 55 were histologically classified as CRPC and 21 as NEPC. We observed that 19/76 (25%) of patients had tumors with high N-Myc expression and *RB1* deletion. Overall 9/55 (16.4%) CRPC and 10/21 (47.6%) NEPC had high N-Myc expression and *RB1* deletion, suggesting that co-occurrence of N-Myc overexpression and *RB1* loss may be enriched for during development of NEPC. Moreover, we observed that high N-Myc expression in combination with *RB1* deletion in patient CRPC and NEPC tumors was significantly associated with a worse overall survival compared to those with high N-Myc expression/*RB1* normal or low N-Myc expression/*RB1* normal (19.93 months (range between 1.83-81.5 months) versus 32.27 (6.6-87.17) or 42.90 (4.2-145.3) months, p=0.03). Our data showed that the co-occurrence of both high N-Myc expression and *RB1* deletion predicted an overall worse prognosis. Several studies have investigated the

role of N-Myc overexpression [1-4] or RB loss [5,6] in driving the development of NEPC, however, the possible synergistic role, if any, of these genetic alterations as drivers has not been reported.

We profiled circulating tumor cells (CTCs) by single-cell whole genome sequencing and immunofluorescence, collected from patients with CRPC and NEPC using the Epic assay (Conteduca et al, NPJ Oncology 2021). We found that while tumor suppressor loss can be seen in advanced prostate cancer patients regardless of histology, co-occurrence of PTEN/RB1/TP53 loss in single CTCs (versus different CTCs) was more common in NEPC. In addition, concurrent tumor suppressor loss was associated with higher NE marker expression and lower AR expression.

We are also profiling plasma cell free DNA (cfDNA) of clinical cohorts to look at tumor genomic alterations and DNA methylation profiles of patients with CRPC and NEPC. As part of this project, we will assess DNA methylation changes associated with MYCN gain and RB1 loss in cfDNA. We will compare cfDNA methylation changes with those observed in GEMM models. Through whole genome bisulfite sequencing, we found overall concordance between tissue and plasma samples including differentially methylated regions in NEPC (hypo-methylated and hyper-methylated sites), as well as methylation of specific neuroendocrine-related genes. We observed patterns in individuals including multiple clones within the circulation with competing frequencies and the dominance of a resistance clones including those with loss of RB1/TP53 (*Beltran et al, JCI, 2020,* PMID 32091413). This data prompted us to expand to a targeted methylation-based assay specifically designed for cfDNA that will allow us to not only assess the presence of NEPC non-invasively but to also correlate cfDNA methylation changes with tumor genomic alterations (eg., MYCN, RB1 ,TP53). This will pave the way for serial assessment to better assess the timing of MYCN in driving NEPC. Development and validation of the targeted cfDNA panel is still ongoing.

2. Specific Aim 2: Assess the impact of timing of N-Myc expression on the development of castration resistance and the NEPC phenotype.

MYCN+ and *Rb1* deletion accelerates progression to AR-negative, poorly differentiated/NEPC tumors, metastases, and decreased median survival.

To determine the impact of N-Myc overexpression and *Rb1* loss on tumor progression *in vivo*, we introduced $Rb1^{f/f}$ alleles into our previously described $Pb\text{-}Cre4^{+/-};Pten^{f/f};LSL\text{-}MYCN^{+/+}$ genetically engineered mouse (GEM) model [3]. For simplicity, we will refer to the different genotypes and controls with aliases (**Figure 2B**). Similar to the clinical cases, both $MYCN+;Rb1^{f/+}$ and $MYCN+;Rb1^{f/f}$ mice had a poorer survival (median survival time of 12.5 weeks ($MYCN+;Rb1^{f/f}$ mice) or 19 weeks ($MYCN+;Rb1^{f/+}$ mice)) compared to *MYCN*+ mice (median survival time of 26 weeks) and $Rb1^{f/f}$ mice (38 weeks, **Figure 2C** [5]). Additionally, $MYCN+;Rb1^{f/f}$ and $MYCN+;Rb1^{f/+}$ mice developed large, invasive tumors with AR-negative and poorly differentiated foci as early as 8 weeks ($MYCN+;Rb1^{f/f}$) or 12 weeks ($MYCN+;Rb1^{f/+}$), respectively. These foci were positive for the neuroendocrine marker INSM1 [7,8], EZH2, as well as NKX2-1, a marker associated with small cell neuroendocrine carcinomas (including prostate) [7-9]. **(Figure 2D, E**). Based on hematoxylin and eosin staining, some of these foci displayed condensed nuclei and scant cytoplasm, characteristics of NEPC morphology. These tumors also included other foci of divergent differentiation (i.e. intestinal and squamous) as well as conventional, AR positive, adenocarcinoma similar to *MYCN*+ primary tumors previously described [2,3] but the percentage of conventional adenocarcinoma decreased over time while the percentage of poorly differentiated histology increased over time. This is in contrast to *MYCN*+ or $Rb1^{f/f}$ tumors, which had primarily high-grade prostatic intraepithelial neoplasia (HGPIN) at the earlier time points.

We also found that the different genotypes were associated with different metastatic potentials (summarized in **Figure 2E**). Lung and liver metastatic lesions were AR negative, however, lymph node metastatic lesions contained both AR positive and negative tumor cells, suggesting that loss of AR expression is not necessary for metastasis. Additionally, both lung and lymph node lesions were RB1-

positive, further suggesting that complete loss of *Rb1* is not necessary to provide metastatic potential. We also found that the onset of metastasis for *MYCN+;Rb1*$^{f/f}$ mice, occurring as early as 8 weeks, was significantly accelerated compared to *MYCN+* [2,3] or *Rb1*$^{f/f}$ [5] mice. By 12 weeks, 100% of *MYCN+;Rb1*$^{f/f}$ intact mice developed distant metastatic lesions (n=8). Metastases to the lung, liver, lymph nodes, and kidney primarily consisted of large and small cell neuroendocrine histologies that stained positive for INSM1 and N-Myc but negative for AR. These data suggest that *Rb1* loss in the context of *MYCN+* accelerates the formation of poorly differentiated tumors with high metastatic potential, and eventually NEPC.

To determine if *Rb1* loss promotes castration resistance in the context of *MYCN+*, we performed longitudinal magnetic resonance imaging (MRI) analyses to track tumor growth before and after castration at 12 weeks of age. Based on both coronal and axial MRI-based tumor volume measurements, *MYCN+;Rb1*$^{f/f}$ mice did not respond to surgical castration and continued to grow rapidly (**Figure 2F**). In contrast, tumors in *Rb1*$^{f/f}$, *MYCN+*, and CTRL mice regressed post-castration. As expected, we found that *MYCN+* and *Rb1*$^{f/f}$ tumors resumed growth 24 weeks post-castration whereas CTRL tumors did not show tumor regrowth at 52 weeks of age, consistent with previous reports [3,5]. In castrated mice, the median survival time was reduced for *MYCN+;Rb1*$^{f/f}$ (24 weeks) compared to *Rb1*$^{f/f}$ (43.5 weeks) and *MYCN+* (44 weeks) mice). In addition, post-castration tumors from *MYCN+;Rb1*$^{f/f}$ mice harbored foci enriched with divergent differentiated histology compared to adenocarcinoma and increased metastatic potential compared to *Rb1*$^{f/f}$ and *MYCN+* mice.

To determine if the local prostate microenvironment is essential for the observed phenotypes, we derived three-dimensional from normal prostate epithelial tissue obtained from 7 to 8-week old *Pb-Cre4*-negative GEMs and transduced them *in vitro* with a Cre-expressing adenovirus. Immunoblot and IHC analyses confirmed the presence of functional alleles following Cre induction and confirmed that all GEM-derived organoids were positive for AR. We injected *MYCN+*^{Cre} and *MYCN+;Rb1*$^{f/fCre}$ organoids subcutaneously into nude mice and monitored allograft tumor growth over time. Tumor volume continuously increased for *MYCN+;Rb1*$^{f/fCre}$ allografts (n=20) from week 3 to 6 while *MYCN+*^{Cre} allografts (n=5) grew at a significantly slower rate which also translated to a significant difference in tumor weights between the groups (p=0.0003). Moreover, *MYCN+;Rb1*$^{f/fCre}$ allograft tumors manifested a similar breakdown and proportion of the different histological patterns to what was observed in primary tumors of *MYCN+;Rb*$^{f/f}$ mice (e.g. AR-positive adenocarcinoma and AR-negative, poorly differentiated foci). Interestingly, allografts from either genotype contained tumor cells that were either AR-negative, weak, or strong, indicating that organoids that were initially AR-positive *in vitro* gradually lost AR expression *in vivo*. However, we observed poorly differentiated foci with NEPC morphology primarily in *MYCN+;Rb1*$^{f/fCre}$ allografts *MYCN+;Rb1*$^{f/fCre}$ allograft growth rate was slightly reduced following castration which is likely due to the fact that the tumors were heterogeneous with a component of AR-responsive adenocarcinoma.

Lastly, lung and lymph node metastatic lesions were only observed in mice bearing *MYCN+;Rb1*$^{f/f}$-Cre allografts (**Figure 2H)**. The majority of metastatic lesions were poorly differentiated although some had squamous and osteoid differentiation. Altogether, these data suggest that *MYCN+;Rb1* loss-induced NEPC morphology, loss of AR expression, and increased metastatic potential are independent of the prostate microenvironment.

N-Myc and *Rb1* genomic loss drives a molecular program consistent with NEPC.

To determine if *MYCN* expression synergizes with *Rb1* loss to drive a molecular program associated with NEPC, we performed RNA-seq on histologically distinct tumor foci ranging from adenocarcinoma to NEPC (**Figure 3A**). Previous studies showed that *TP53* mutations can synergize with *RB1* loss to drive a phenotype similar to what we observed in the *MYCN+;Rb1*$^{f/f}$ mice [5,6,10].Therefore, we first queried our RNA-seq data for spontaneous mutations in *Trp53* and in *Rb1*. All single nucleotide variants (SNVs) and insertions/deletions (indels) in the *Trp53* and *Rb1* genes were profiled for each histopathological subtypes of mouse tumors across all genotypes (**Figure 3B**). We observed exonic non-silent mutations in *Trp53* exons and synonymous exonic mutations in *Rb1*. Of the *Trp53* alterations, we

noted a missense mutation (c.T715G) in exon 7 within the DNA binding domain. This mutation is equivalent to C242R in the human *TP53* gene (obtained from Vista-Point tool [11,12]) and was found to have a moderate effect (Ensembl Variant Effect Predictor) to deleterious (SIFT) or damaging (PolyPhen) [13,14] impact on TP53 function. The other *Trp53* mutation (c.157dupT) was a frameshift insertion in exon 4 in the linker domain and the human equivalent (W53Cfs*4) was observed to have high impact on TP53 function (Ensembl Variant Effect Predictor). Both human mutations were found in the COSMIC database of mutations, however, none of the observed variants in either gene were specific for poorly differentiated or NEPC tumors in mice irrespective of genotype.

A previously described NEPC score estimates the likelihood a test sample is clinical NEPC based on a set of 70 differentially expressed NEPC-related genes [15]. We calculated the NEPC score for each tumor focus and found that adenocarcinoma foci did not score significantly different from wild type prostates (data not shown). Furthermore, poorly differentiated tumor foci had significantly higher NEPC scores compared to conventional adenocarcinoma and were similar to values obtained from a cohort of patient NEPC tumors ($p < 0.0001$, **Figure 3C**). Interestingly, tumor foci with divergent differentiation (squamous, poor, osteoid) from castrated mice also had NEPC scores similar to clinical NEPC and were significantly higher than adenocarcinoma of intact tumors ($p=0.0034$). This suggests that castration results in the activation of an NEPC molecular program regardless of histology.

We then compared the expression differences between distinct histological tumor foci to identify differentially expressed pathways associated with accelerated tumor progression. Ward's hierarchal clustering was performed using a 2,043 gene signature that distinguished *MYCN+;Rb1*$^{f/f}$ poorly differentiated/NEPC foci from *MYCN+* adenocarcinoma foci (adj. $p<0.05$, $|(\text{Log}_2 \text{ (Fold Change)}| > 2$), which revealed three distinct sets of gene clusters (**Figure 3D)**. Genes found in clusters 1 and 2 were highly upregulated in poorly differentiated and NEPC-like samples and were enriched with E2F and MYC targets, PRC2 complex, cell cycle, neural lineage and EMT genes (**Figure 3E, F**). Adenocarcinoma foci were enriched with EMT, PRC2 complex and AR signaling/prostate developmental genes. Interestingly, we observed an enrichment of a loss TP53 signaling in poorly differentiated tumor foci compared to adenocarcinoma despite no distinguishing loss of function mutations or change in *Trp53* expression (**Figure 3B**).

3. Specific Aim 3: Determine the impact of the timing of N-Myc on response to NEPC directed therapeutics.

Single Cell-Based Approaches Reveal NEPC-Like Subpopulations.

We next sought to characterize the temporal evolution of tumors in *Rb1*$^{f/f}$ and *MYCN+;R1b*$^{f/f}$ mice. To this end, we performed IHC staining on prostate tissues from 8-week old mice and found that while prostates from *Rb1*$^{f/f}$ mice were composed of AR-positive, HGPIN lesions, tumors from *MYCN+;Rb1*$^{f/f}$ mice contained large regions of AR-positive adenocarcinoma as well as neighboring foci comprised of AR-negative, INSM1-positive cells (**Figure 4A**). In order to better understand this heterogeneity we observed in the developing tumors, we performed single cell RNA sequencing (scRNA-seq) on prostates collected from 8-week old *MYCN+;Rb1*$^{f/f}$ mice as well as age-matched *Rb1*$^{f/f}$ mice and sought to identify subpopulations that may contribute to tumorigenesis. K-means clustering and UMAP projection of the combined data across both genotypes revealed 10 major cell clusters of gene expression (**Figure 4B**). Differential expression analysis between clusters produced a list of the top 50 most differentially expressed genes by cluster (**Figure 4C**), and we assigned identities to each cluster using the expression of known markers (**Figure 4B**). We restricted further analyses to include populations which were identified as luminal epithelium, basal epithelium or neuroendocrine cells on the basis of *Krt5, Krt8, Cd24a, Trp63,* and *Insm1* expression. Re-clustering of this subset allowed for further delineation of the heterogeneity within these populations (*Rb1*$^{f/f}$ mice: 8,151 cells; *MYCN+;Rb1*$^{f/f}$ mice: 5,160 cells) (**Figure 4D**). We then assessed what proportion of each cluster was comprised of cells from each genotype and found striking differences in composition (**Figure 4E**). Using gene expression, we identified a population of cells in *Rb1*$^{f/f}$ tumors that

were positive for the luminal markers *Ar* and *Cd24a* as well as had high levels of AR signaling activity assessed by *Fkbp5* expression (**Figure 4F**). This population was markedly reduced in *MYCN+;Rb1$^{f/f}$* tumors and instead there was an abundance of cells that expressed *Ezh2* and had low levels of AR signaling activity, suggesting a transition away from an AR-dependent state (**Figure 4F**). These data are consistent with previous findings that have shown that N-Myc and EZH2 cooperate to suppress AR signaling [2,3]. Furthermore, the *Ezh2*-positive/AR-signaling low population also had increased expression of a previously published adult stem cell (ASC) signature score [16] and expression of *Sox2*, consistent with the transition away from an adenocarcinoma state (**Figure 4F**). Interestingly, we also identified a population of cells which expressed a number of known neuroendocrine markers, including *Ascl1*, *Chga*, *Foxa2*, and *Insm1* (**Figure 4F**). The ASC signature score was significantly higher in *MYCN+;Rb1$^{f/f}$* tumors compared to *Rb1$^{f/f}$* tumors (**Figure 4G**) and was found to be enriched in the cluster containing neuroendocrine cells (**Figure 4H**).

Cell Trajectories Towards a Neuroendocrine-Like Lineage.

In order to understand the transcriptional relationships between the epithelial and neuroendocrine cell populations, we employed a computational method (Monocle) [17] to define cell trajectories between the given lineage states. Clustering of the cells derived from *MYCN+;Rb1$^{f/f}$* tumors alone again revealed three distinct cell populations consisting of basal and luminal epithelium as well as a neuroendocrine population on the basis of *Krt5, Krt8, Cd24a, Trp63,* and *Insm1* expression (**Figure 5A**). Cell trajectories and UMAP projections highlighted the existence of a transition between luminal epithelial cells and neuroendocrine cells (**Figure 5B**). This was further confirmed by assessing the expression of known marker genes as a function of pseudotime distance from the neuroendocrine population. Keratin 5 (*Krt5*), a known basal epithelial cell marker, was highly expressed in cells with the greatest pseudotime distance from the neuroendocrine population and was largely restricted to the basal epithelial cell population (**Figure 5C**). Levels of *Ar* and its target gene *Tmprss2* were highly expressed in luminal and basal populations and showed low levels of expression in the neuroendocrine population (**Figure 5C**). Robust levels of *Ezh2* were observed throughout all cells, with a modest increase of expression in the neuroendocrine population (**Figure 5C**). As expected, neuroendocrine markers such as *Ascl1*, *Insm1*, *Foxa2*, and *Chga* were all highly expressed in the neuroendocrine population (**Figure 5C**). Surprisingly, this analysis revealed small populations of cells in the luminal epithelial cluster which were beginning to express these neuroendocrine markers, despite being a significant pseudotime distance away from the neuroendocrine population (**Figure 5C**). While the terminal neuroendocrine state also existed in *Rb1$^{f/f}$* tumors, the appearance of these early-transition cells occurred with higher frequency and at an earlier point in pseudotime in *MYCN+;Rb1$^{f/f}$* tumors and suggests that this approach can potentially identify cells early in a transition to a neuroendocrine state (**Figure 5C**). We then took an unbiased approach to identify gene modules which were differentially expressed as a function of pseudotime. We identified 22 modules whose expression levels correlated with the three cell states (**Figure 5D**). GSEA performed on the genes from the most highly expressed module in each cluster revealed differences between the clusters, most notably including enrichment of EZH2-related developmental and neural gene sets in the neuroendocrine cluster (cluster 3, **Figure 5E**). The projection of the expression score of the three most highly expressed modules corresponded, as expected, to the three cell states on which they were defined (**Figure 5F**). Intriguingly, while modules 9 and 20 were fairly restricted to luminal and basal populations respectively, module 19 was highly expressed in the neuroendocrine cells as well as a subset of luminal cells that were closest to the neuroendocrine population on the computed cell trajectory (**Figure 5F**). The corresponding module in *Rb1$^{f/f}$* tumors, while able to identify the neuroendocrine population, did not show a marked enrichment in the cells contained in the luminal population that were along the computed cell trajectory (**Figure 5**).

To better understand the evolution of the cells expressing neuroendocrine markers, we performed scRNA-seq at an earlier time point (6 weeks of age). At this age, prostates of *MYCN+;Rb1$^{f/f}$* mice contained primarily HGPIN as well as foci of AR-/INSM1- invasive carcinoma .Based on a combined analysis of luminal and neuroendocrine cells in the 6- and 8-week scRNA-seq data, we uncovered two distinct clusters of cells that were AR negative and displayed intermediate to high levels of neuroendocrine marker gene

expression (*Insm1*) as well as ubiquitin C-terminal hydrolase L1 (*Uchl1*) (**Figure 5G**). Moreover, these two populations were distinguished by differential expression of *Ascl1/Chga* versus the Oct11-encoding gene *Pou2f3* that is also overexpressed in a subset of clinical CRPC and NEPC tumors (**Figure 5G**). These populations were observed in both 6-week and 8-week timepoints and the cells from both timepoints contributed to all clusters. We next sought to identify genes that marked the intermediate population of cells that were transitioning towards a neuroendocrine phenotype. We performed a differential expression analysis and identified 1,822 genes which were significantly enriched in the cluster of cells found between the luminal and neuroendocrine populations, including *Pou2f3*, *Ovol3*, and *Ascl2* (**Figure 5**).

To determine the clinical relevance of these findings, we performed similar scRNA-seq based approaches on a clinical sample isolated from a patient of Dr. Beltran who presented with an AR-positive prostate adenocarcinoma and AR-negative NEPC liver metastasis. Genomic profiling of the primary tumor identified a 5.8Mb focal deletion of *PTEN* (10:89,536,129-90,122,394) and missense mutation in *TP53* (R273C). While the NEPC liver metastasis shared the *PTEN* deletion with the primary tumor and also harbored a missense mutation in *TP53* (R114C), the metastatic lesion carried a nonsense mutation and predicted loss-of-function of *RB1* (R579X) .The patient progressed following androgen deprivation therapy, docetaxel, and carboplatin treatment and developed an NEPC pleural effusion that was isolated and subjected to scRNA-seq. Analysis of the scRNA-seq data revealed numerous subclusters within the main tumor cell population after removal of hematopoietic and stromal populations (**Figure 5H**). Gene Ontology analysis of the differentially expressed genes between the clusters revealed populations that were enriched for varying cellular processes, including DNA damage response and neural lineage pathways. Similar to the genetic context of the mouse models, the NEPC patient sample contained a substantial number of *MYCN*-positive/*RB1*-negative cells (**Figure 5H**). We also observed a high number of *EZH2*+/AR signaling low cells (**Figure 5H**), many of which also expressed *SOX2* (**Figure 5H**) and *UCHL1*, consistent with our findings in *MYCN+;Rb1*$^{f/f}$ mice. Finally, application of the ASC signature score [16] revealed a strong overlap with cells positive for the marker *MKI67,* indicating the enhanced proliferative capacity of this population . We also performed scRNA-seq on a second prostate cancer sample from a patient who developed a local recurrence in the prostate with mixed small cell carcinoma and adenocarcinoma following ADT treatment. Consistent with our findings in *MYCN+;Rb1*$^{f/f}$ mice, we found a cluster of cells which were strongly positive for the neuroendocrine marker genes *INSM1* and *CHGA* as well as *SOX2* and *UCHL1* in addition to a large cluster of cells which showed marked reduced expression of these genes. RNA velocity analysis of these two populations revealed the existence of cell trajectories which would suggest that cells would most likely transition towards the neuroendocrine cluster.

Distinct Chromatin Accessibility Patterns Exist in Neuroendocrine Subpopulations.

Based on the transcriptional heterogeneity observed during tumorigenesis and the existence of cell trajectories that suggested lineage plasticity between luminal epithelium and neuroendocrine cells, we sought to identify the factors that may be responsible for promoting this change in lineage state. To this end, we performed single cell assay for transposase-accessible chromatin followed by sequencing (scATAC-seq) to determine regions of differential chromatin accessibility between populations. Following library generation and sequencing, fragment sizes varied with a periodicity roughly corresponding to nucleosome spacing (**Figure 6A**). As expected, regions with the highest levels of accessibility were centered around the transcription start site (TSS) of genes (**Figure 6B**). After clustering the chromatin accessibility data, we assessed accessibility at a number of lineage-specific loci (such as *Krt8*, *Psca*, *Ascl1*, *Ptprc*, *Col3a1*, and *Pecam1*) to assign identities (luminal, basal, neuroendocrine, stroma) to the cells. Moreover, we observed distinct subclusters among the basal, luminal, and neuroendocrine populations (**Figure 6C**). The two neuroendocrine subclusters demonstrated high accessibility at known neuroendocrine marker gene loci, therefore we performed a differential accessibility analysis between the NE1 and NE2 populations to uncover differences between these two cluste. From this comparison, we found that the NE1 population had an enrichment of chromatin accessibility at the *Foxa2* locus while the NE2 population had a significant enrichment at the *Ascl2* and *Pou2f3* loci (**Figure 6D**), similar to the scRNA-seq data (**Figure 5G**). In contrast, the genomic loci for *Ar* and the AR target gene *Tmprss2* showed high levels of accessibility

in all luminal and basal populations and virtually no accessibility in either of the neuroendocrine populations (**Figure 6D**). We identified regions of chromatin with differential accessibility between all the subpopulations and performed motif analyses to determine the transcription factor binding sites which were enriched in the hyper-accessible and hypo-accessible regions. As expected, luminal populations were enriched for GATA motifs along with glucocorticoid response elements (GRE) and androgen response elements (ARE) (**Figure 6E**). Interestingly, the neuroendocrine populations were characterized by differential enrichment of ASCL1 motifs in the NE1 population and of OCT/POU family members in the NE2 population (**Figure 6E**), consistent with differences seen in accessibility at the *Pou2f3* loci (**Figure 6D**). In agreement with our scRNA-seq findings, these data suggest the existence of discrete neuroendocrine populations which may be driven by distinct transcriptional programs.

The N-Myc Cistrome Is Altered Upon *Rb1* Loss.

Based on single-cell based sequencing data from the GEMs, we observed that the overexpression of *MYCN* in combination with the loss of *Rb1* resulted in the rapid formation of aggressive, metastatic tumors with neuroendocrine-like features. Thus, we hypothesized that the loss of *Rb1* would synergize with *MYCN* overexpression to reshape the N-Myc cistrome and drive tumor progression. To address this, we performed N-Myc chromatin immunoprecipitation sequencing (ChIP-seq) on multiple, independent tumors collected from *MYCN*+ or *MYCN+;Rb1*$^{f/f}$ mice. Consistent with its role as a transcription factor, N-Myc binding was highly enriched near the transcription start site (TSS) of genes in both genotypes. We found 36,789 N-Myc peaks in *MYCN*+ tumors, in relative agreement with our previous studies of N-Myc binding in human prostate cancer cells [2]. Surprisingly, following the loss of *Rb1*, the N-Myc cistrome was dramatically expanded to 62,171 binding sites with nearly 60% of these sites corresponding to new binding sites not seen in *MYCN*+ mice alone (**Figure 7A**). Additionally, GSEA of the *MYCN*+ and *MYCN+;Rb1*$^{f/f}$ unique peaks revealed distinct sets of genes bound by N-Myc between the conditions. While many luminal epithelial and hormone-responsive gene sets were enriched in *MYCN*+ tumors, a large enrichment of PRC2 complex targets, epigenetically marked developmental, and neural lineage gene sets was found in *MYCN+;Rb1*$^{f/f}$ tumors. To determine the transcriptional co-factors which may contribute to this differentially remodeled cistrome, we performed motif enrichment analysis between N-Myc peaks unique to the *MYCN*+ and *MYCN+;Rb1*$^{f/f}$ mice. While the most differentially enriched motifs in *MYCN*+ tumors consisted of TP53 and ARE motifs, *MYCN+;Rb1*$^{f/f}$ tumors were enriched for ASCL and SNAIL family motifs (**Figure 7B**). More strikingly, a high degree of enrichment was observed for a motif consistent with the E2F family of transcription factors [18] (**Figure 7B**). To assess the degree of altered N-Myc binding and chromatin accessibility, we integrated the scATAC-seq and the ChIP-seq data and restricted the analysis to regions of differential accessibility between subpopulations. In the presence of wild-type levels of *Rb1*, N-Myc was bound at regions of accessible chromatin associated with luminal populations (**Figure 7C**). In the context of *Rb1* loss, N-Myc binding was reduced in the luminal-specific regions and instead was dramatically enriched in regions which were accessible only in the neuroendocrine populations (**Figure 7C**). Specifically, we found that N-Myc binding was reduced at the *Ar* locus and redirected to neuroendocrine-associated genes, such as *Ascl1* and *Insm1*, in *MYCN+;Rb1*$^{f/f}$ tumors (**Figure 7D**). Importantly, the loss of *Rb1* appeared to remodel the N-Myc cistrome in a very specific manner, as binding at the *Gapdh* locus (a known N-Myc target gene) remained consistent between *MYCN*+ and *MYCN+;Rb1*$^{f/f}$ tumors (**Figure 7D**). Together, these data suggest that the loss of *Rb1* synergizes with N-Myc overexpression to redirect the N-Myc cistrome to new genomic loci to regulate gene expression, possibly with the help of ASCL- and E2F-family members.

Determine the impact of the timing of N-Myc on response to NEPC directed therapeutics.

We have tested our PTEN/MYCN and PTEN/MYCN/RB1 models as well as patient-derived NEPC organoids with monotherapies and combination therapies to determine the impact of MYCN and EZH2 status on response to NEPC-directed therapeutics. We observe variable response to single agent EZH2 inhibitor therapy (tazemetostat) in our mouse and patient-derived models. While expression of MYCN did

not correlate with response, we are expanding our studies to additional patient-derived models (recently published --Tang et al Science 2022) and are exploring other mediators of response and resistance using transcriptome and ChiPseq analyses. Post-treatment transcriptome data has pointed to potential targets for combination therapy including ALK and NRTK which we are now testing, in addition to alisertib described in our organoid drug screen.

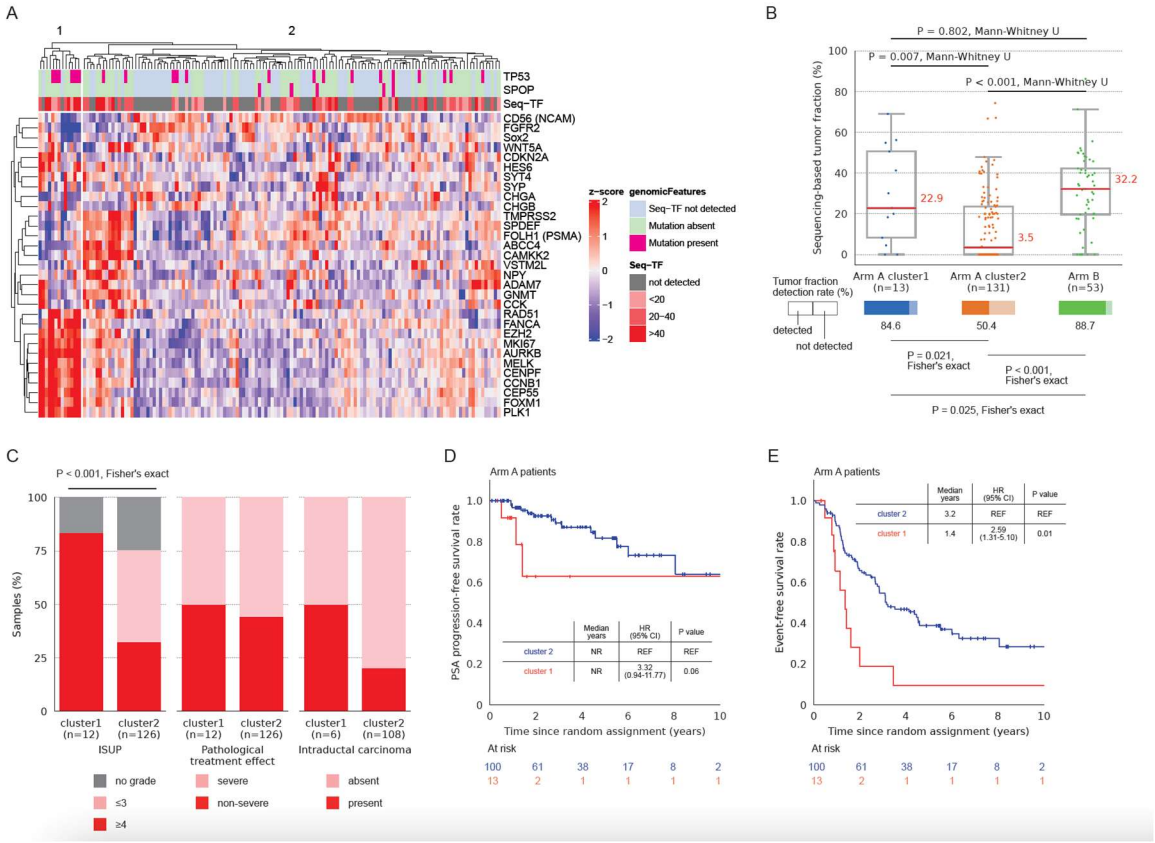

Figure 1. Gene expression analysis of prostatectomy samples from CALGB 90203. (A) Hierarchical clustering heatmap analysis of Differentially expressed genes (DEGs) between DNA sequencing determined tumor fraction (Seq-TF) detected (n=77) versus not detected (n=67) within Arm A (neoadjuvant therapy) revealed two clusters (1 and 2) (P-value=0.03857). Red in the heatmap denotes upregulation while blue denotes downregulation. Horizontal axis is the samples in Arm A and the vertical axis denotes the DEGs based on Seq-TF status. The dendrogram values are measured by Euclidean distance with a complete linkage clustering algorithm. **(B)** Box plot shows the Seq-TF in samples from Arm A cluster1, Arm A cluster2, and Arm B (untreated). At the bottom of the plot, horizontal blue, orange, or green filled rectangles illustrate the proportion of samples in each group that had evidence of residual tumor DNA by sequencing. **(C)** Association between clusters and clinical outcomes in patients with high risk localized PCa exposure to chemohormonal therapy. **(D)** and **(E)** Kaplan–Meier survival analysis for PSA progression free survival and event-free survival in patients between 2 clusters identified based on Seq-TF status in Arm A. P values were estimated using a Pearson's Chi-squared test with Yates' continuity correction, Fisher's Exact Test, Mann-Whitney U test (A, B, C), or univariate Cox proportional hazards regression analysis (D, E).

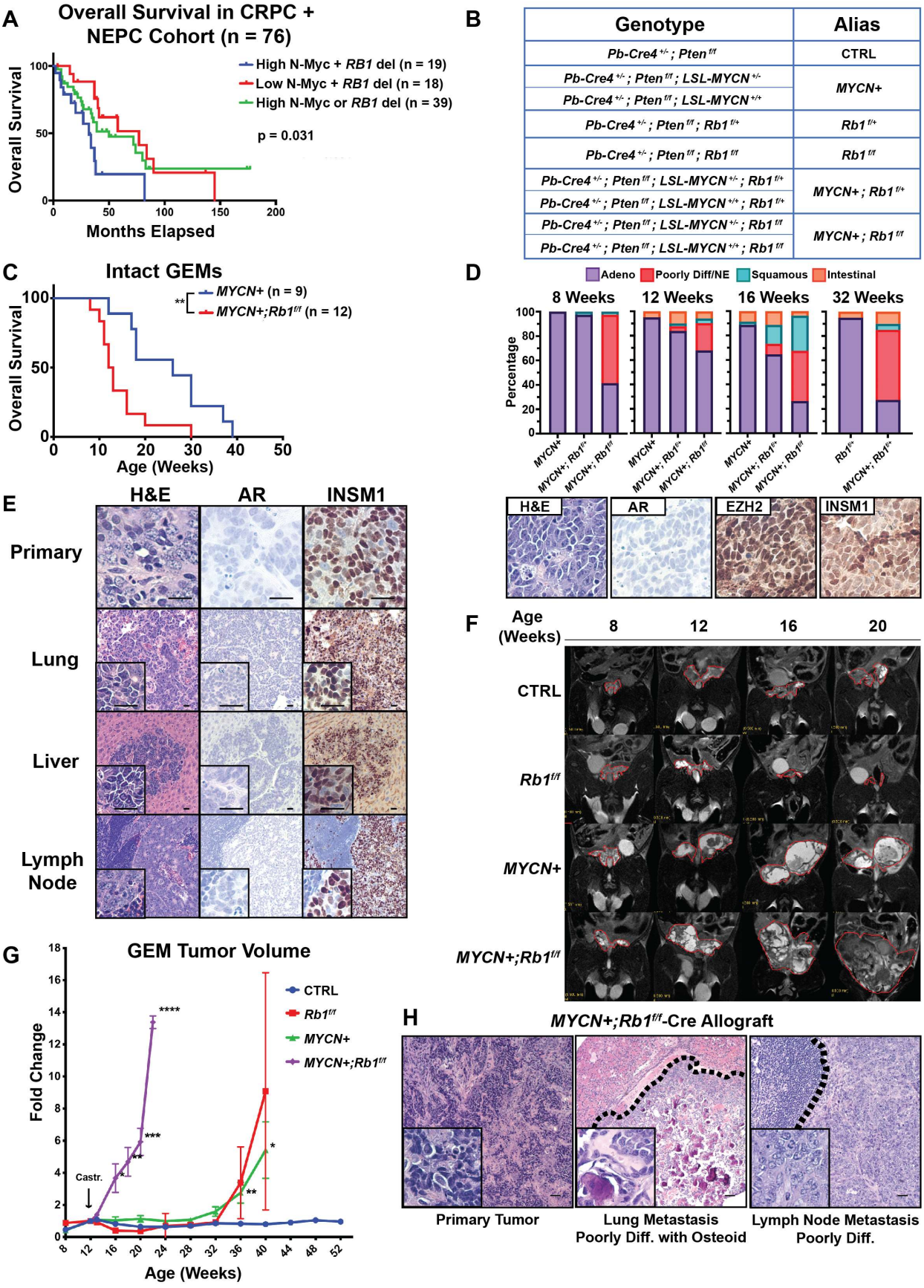
A
Overall Survival in CRPC + NEPC Cohort (n = 76)
High N-Myc + RB1 del (n = 19)
Low N-Myc + RB1 del (n = 18)
High N-Myc or RB1 del (n = 39)
p = 0.031
Overall Survival
Months Elapsed
B
Genotype
Alias
Pb-Cre4 +/- ; Pten f/f
CTRL
Pb-Cre4 +/- ; Pten f/f ; LSL-MYCN +/-
Pb-Cre4 +/- ; Pten f/f ; LSL-MYCN +/+
MYCN+
Pb-Cre4 +/- ; Pten f/f ; Rb1 f/+
Rb1 f/+
Pb-Cre4 +/- ; Pten f/f ; Rb1 f/f
Rb1 f/f
Pb-Cre4 +/- ; Pten f/f ; LSL-MYCN +/- ; Rb1 f/+
Pb-Cre4 +/+ ; Pten f/f ; LSL-MYCN +/+ ; Rb1 f/+
MYCN+ ; Rb1 f/+
Pb-Cre4 +/- ; Pten f/f ; LSL-MYCN +/- ; Rb1 f/f
Pb-Cre4 +/+ ; Pten f/f ; LSL-MYCN +/+ ; Rb1 f/f
MYCN+ ; Rb1 f/f
C
Intact GEMs
MYCN+ (n = 9)
MYCN+;Rb1f/f (n = 12)
Overall Survival
Age (Weeks)
D
Adeno
Poorly Diff/NE
Squamous
Intestinal
8 Weeks
12 Weeks
16 Weeks
32 Weeks
Percentage
MYCN+
MYCN+; Rb1f/+
MYCN+; Rb1f/f
Rb1f/+
MYCN+; Rb1f/+
H&E
AR
EZH2
INSM1
E
H&E
AR
INSM1
Primary
Lung
Liver
Lymph Node
F
Age (Weeks)
8
12
16
20
CTRL
Rb1f/f
MYCN+
MYCN+;Rb1f/f
G
GEM Tumor Volume
CTRL
Rb1f/f
MYCN+
MYCN+;Rb1f/f
Fold Change
Castr.
Age (Weeks)
H
MYCN+;Rb1f/f-Cre Allograft
Primary Tumor
Lung Metastasis
Poorly Diff. with Osteoid
Lymph Node Metastasis
Poorly Diff.

Figure 2. *MYCN+* and *RB1* deletion accelerates progression to NEPC. A. Kaplan-Meier plots of CRPC (n=55) and NEPC (n=21) patients stratified into three categories according *MYCN* (N-Myc) expression and/or *RB1* status. Univariate overall survival analysis was calculated from the time of initial diagnosis of metastatic disease to death from any cause. Patients still alive at time of last follow-up were censored. Patients with high N-Myc expression and *RB1* deletion showed significantly worse survival compared to the other two groups (p=0.031, Kaplan-Meier estimator (log-rank test). **B.** Table of genotype aliases used. **C.** Survival plots of intact *MYCN+* or *MYCN+;Rb1$^{f/f}$* mice using the Kaplan-Meier estimator (log-rank test). **D.** Top: percentage of GEM tumor foci with conventional adenocarcinoma (including HGPIN, intracystic carcinoma, adenocarcinoma), poorly differentiated/neuroendocrine features, squamous differentiation, and intestinal differentiation based on pathologist assessment. Bottom: Hematoxylin and eosin (H&E) and IHC staining of NEPC focus for N-Myc, RB1, epithelial markers AR and CK8, reprogramming factor EZH2, and small cell neuroendocrine marker INSM1. Scale bar: 50 μm. **E.** H&E and IHC of AR, N-Myc, INSM1 on primary tumor, lung, liver, and lymph node metastasis in a *PbCre$^{+/-}$; Pten$^{f/+}$; MYCN$^{+/+}$; Rb1$^{f/f}$* 19-week-old mouse. Scale bar: 50 μm. **EF** MRI coronal scans from CTRL (n=5), *Rb1$^{f/f}$* (n=3); *MYCN+* (n=4); and *MYCN+;Rb1$^{f/f}$* (n=6) GEMs from 8 to 20 weeks of age. Mice were castrated at 12 weeks of age. **G.** Fold change volume over time of GEM tumors from mice castrated at 12 weeks. *p<0.05, **p<0.01, ***p<0.001, ****p<0.0001. **H.** H&Es of poorly differentiated subcutaneous mouse allograft primary tumor and metastases derived from Adeno-Cre-transduced *MYCN+;Rb1$^{f/f}$* organoids. The dashed lines separate the tumor metastasis from normal tissue. Scale bar: 50 μm.

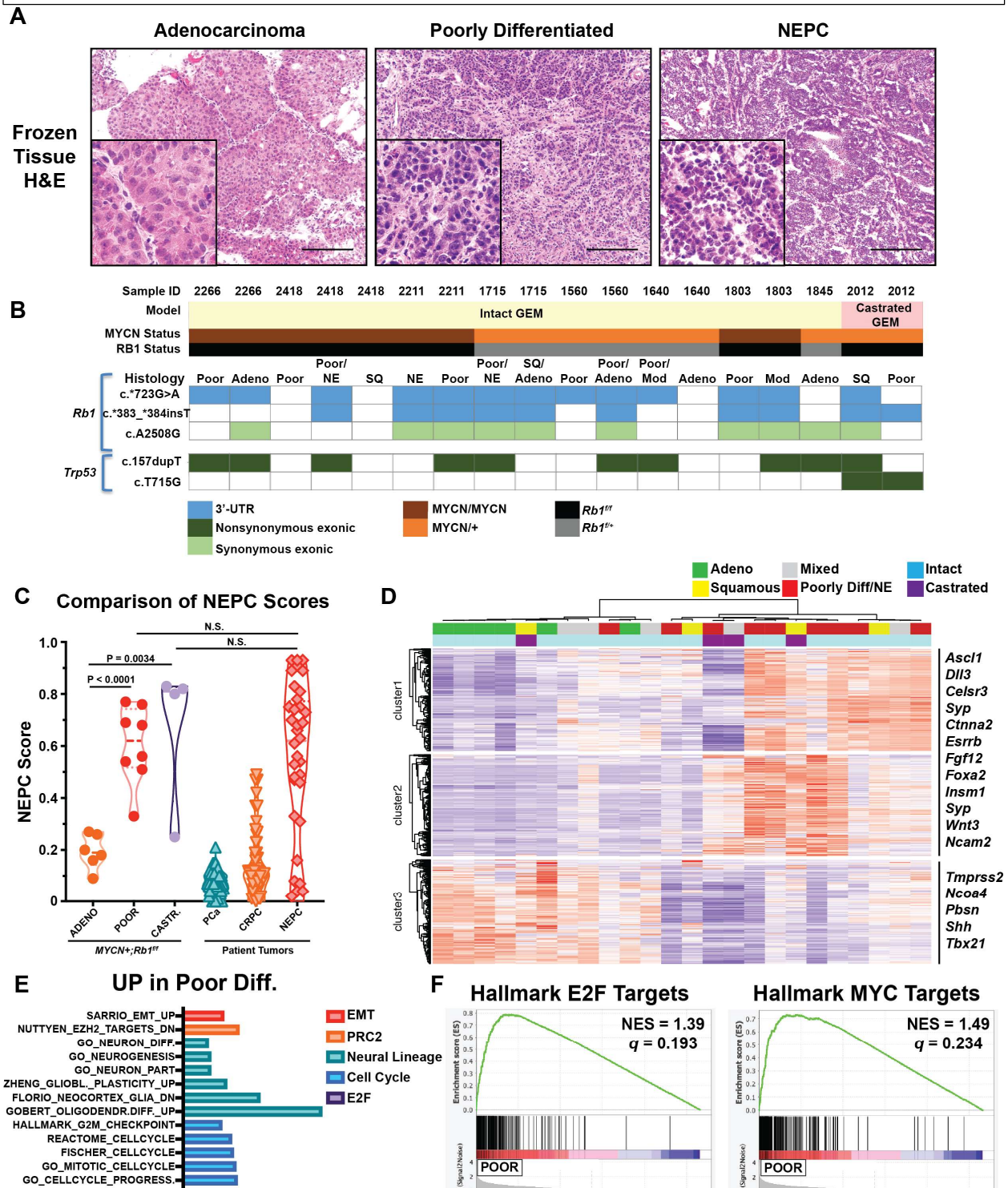

Figure 3. Poorly differentiated tumors have molecular signatures similar to clinical NEPC. A. H&E from frozen tumors showing examples of adenocarcinoma, poorly differentiated, and NEPC histology. Scale bar: 50 μm. **B**. Single nucleotide variants and indels at *Trp53* and *Rb1* in mouse tumors from RNA-seq data. **C.** Left: Violin plot of NEPC scores from *MYCN+;Rb1*$^{f/f}$ GEMs with conventional adenocarcinoma and poorly differentiated/NEPC histologies, as well as PCa, CRPC, and NEPC patient samples. **D.** Heatmap and hierarchal clustering of poor, squamous, adenocarcinoma and mixed differentiation foci from GEMs based on the *MYCN+;Rb1*$^{f/f}$ POOR vs. *MYCN+* ADENO Signature. **E.** Top gene sets related to E2F targets, cell cycle, neuronal development, epigenetic reprogramming, epithelial identity, p53 targets, and AR signaling. UP: log2FC > 1.5 DOWN: log2FC < -1.5, p < 0.05. **F.** GSEA enrichment plots of Hallmark E2F Targets and Hallmark MYC Targets in poorly differentiated (POOR) vs. adenocarcinoma (ADENO).

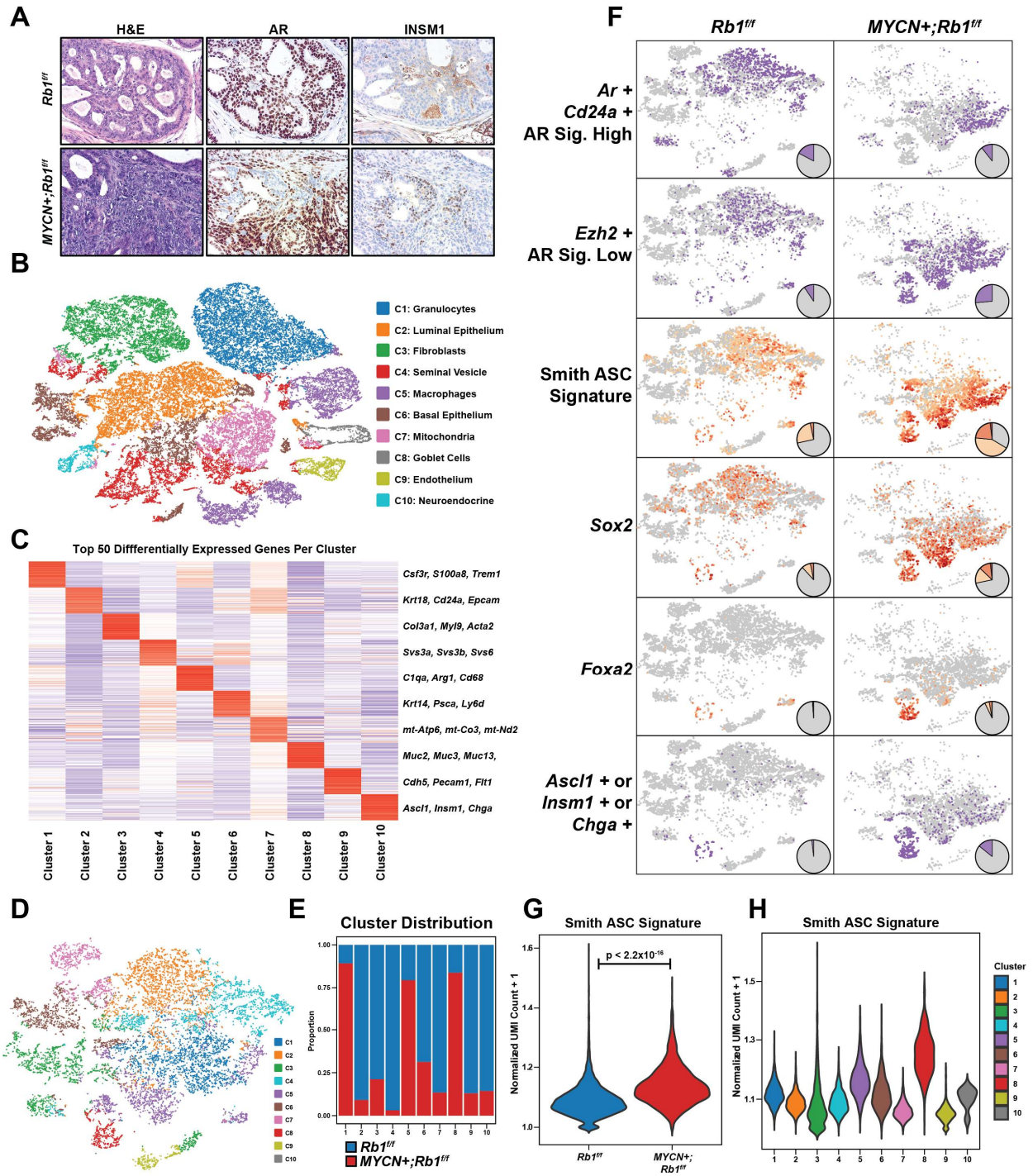

Figure 4. Single cell-based approaches reveal NEPC-like subpopulations. A. H&E and IHC staining of AR and INSM1 in samples used for scRNA-seq. **B.** Combined t-SNE plot of scRNA-seq data from *Rb1*$^{f/f}$ (n=3) and *MYCN+;Rb1*$^{f/f}$ (n=3) mice. **C.** Clustering of the top 50 most differentially expressed genes between clusters. **D.** Reclustering of combined luminal, basal and neuroendocrine populations from *Rb1*$^{f/f}$ (n=3) and

MYCN+;Rb1$^{f/f}$ (n=3) mice. **E.** Distribution of genotypes between clusters identified in panel D. **F.** Expression of indicated markers or signature in *Rb1*$^{f/f}$ (n=3) compared to *MYCN+;Rb1*$^{f/f}$ (n=3) mice. Pie charts show proportions of positive vs. negative cells or high/medium/low/negative gene expression. **G.** Violin plot of Smith ASC score [16]. **H.** ASC score by cluster from panel D.

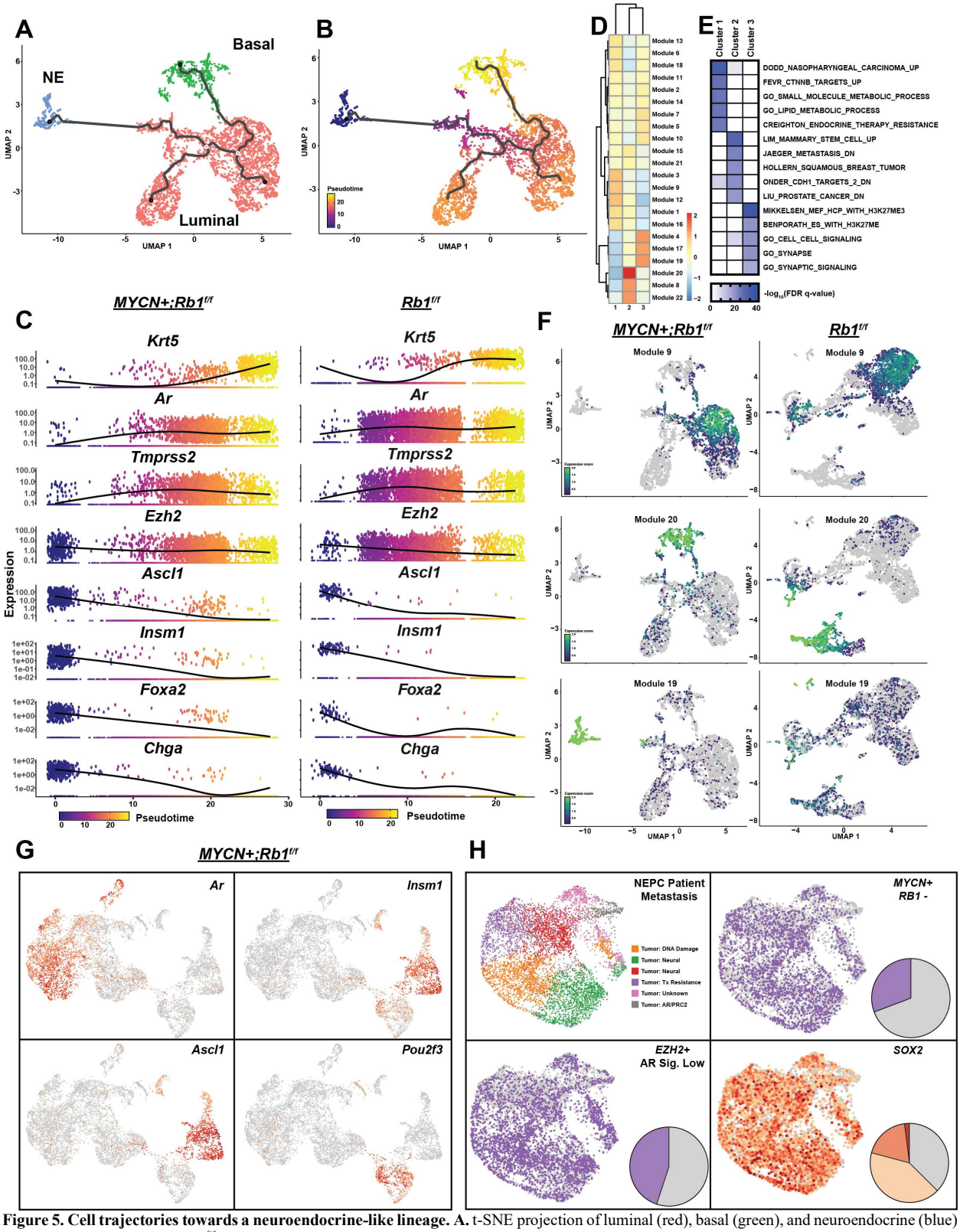

Figure 5. Cell trajectories towards a neuroendocrine-like lineage. A. t-SNE projection of luminal (red), basal (green), and neuroendocrine (blue) populations from *MYCN+;Rb1*$^{f/f}$ mice (n=3). **B.** Pseudotime trajectories projected onto t-SNE from panel A. **C.** Gene expression levels of indicated

genes over pseudotime (neuroendocrine population located at t=0) in *MYCN+;Rb1*$^{f/f}$ (left) and *Rb1*$^{f/f}$ (right) mice. **D.** Heatmap and clustering of gene expression modules which vary significantly as a function of pseudotime in *MYCN+;Rb1*$^{f/f}$ mice. **E.** GSEA results showing the top 5 gene set enriched in modules 9, 19, and 20. **F.** Expression of genes from modules 9, 19 and 20 projected onto *MYCN+;Rb1*$^{f/f}$ (left) and *Rb1*$^{f/f}$ (right) mice. **G.** Expression of indicated genes in luminal and neuroendocrine cells of 6-week-old (n=2) and 8-week-old (n=3) *MYCN+;Rb1*$^{f/f}$ mice. **H.** UMAP of scRNA-seq data from a metastatic NEPC sample. Clusters were named based on GSEA results of differentially expressed genes between clusters.

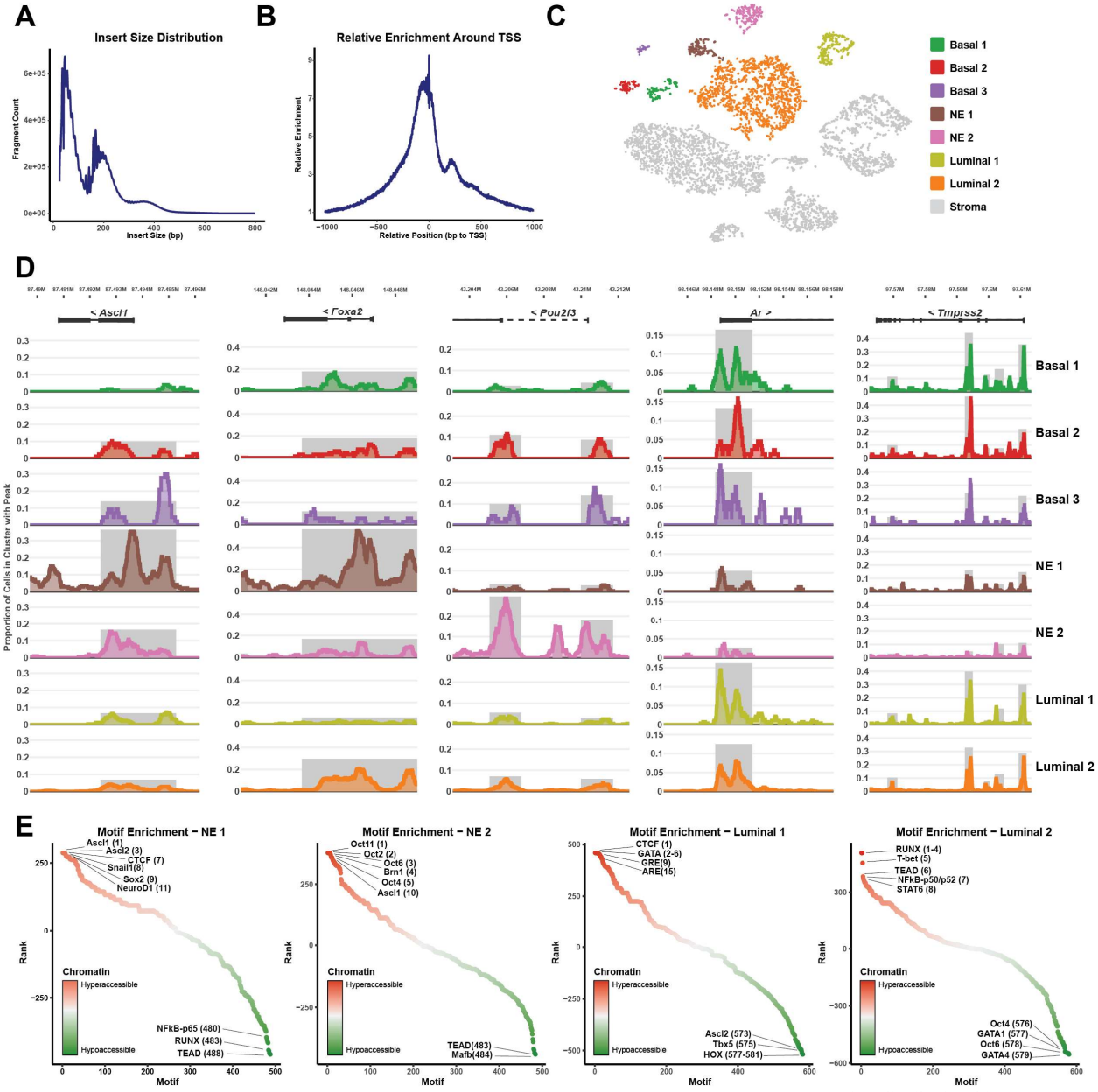

Figure 6. Distinct chromatin accessibility patterns exist in neuroendocrine subpopulations. A. Insert size distribution histogram from scATAC-seq data revealing expected nucleosome spacing. **B.** Histogram depicting the relative enrichment of accessible chromatin centered at the transcription start site (TSS) of genes. **C.** t-SNE plot of scATAC-seq data from *MYCN+;Rb1*$^{f/f}$ mice. **D.** Chromatin accessibility in the subpopulations at the indicated loci. **E.** Graphs of differential transcription factor motif enrichment in the indicated subpopulations called on regions of hyper- and hypo-accessible chromatin between clusters.

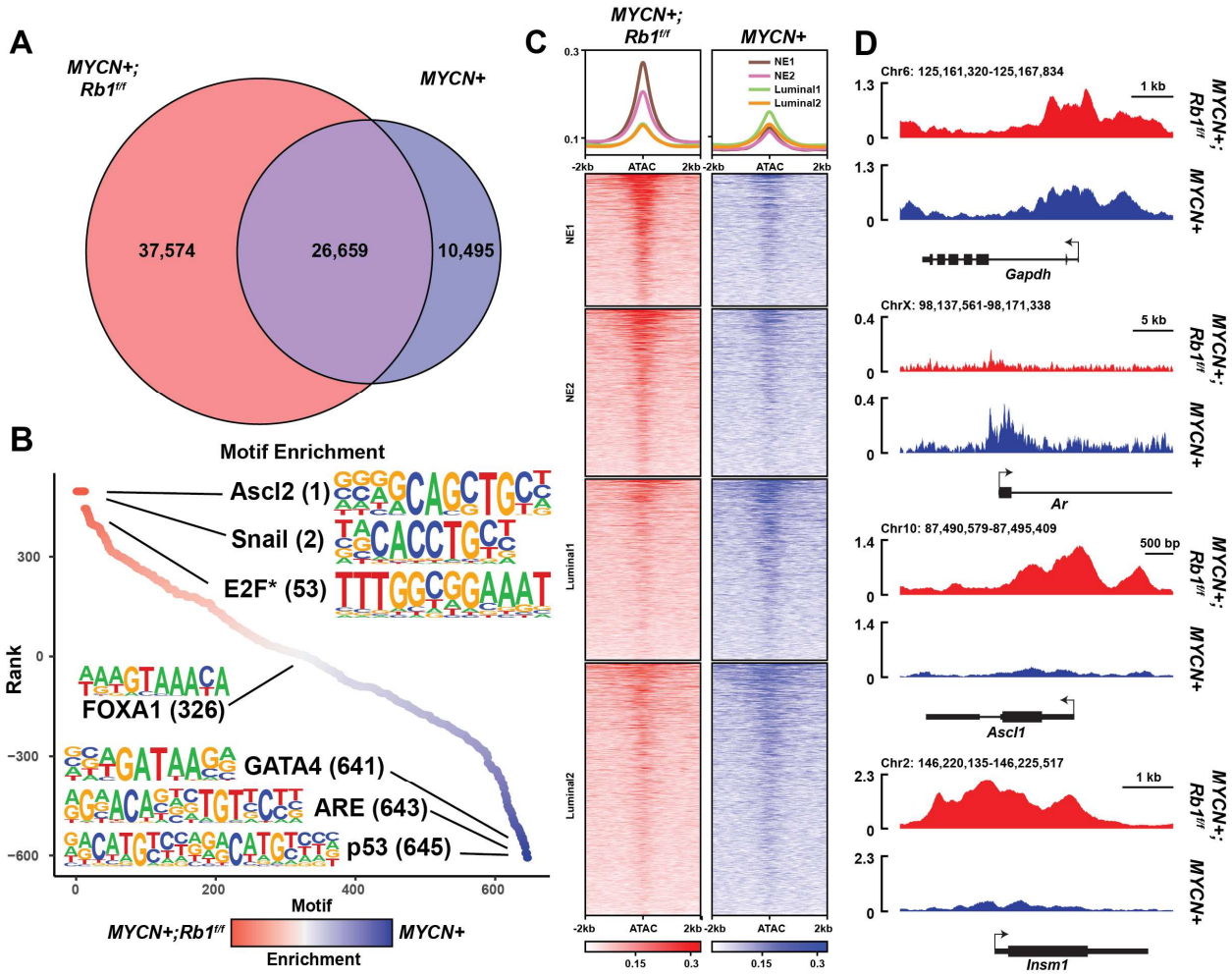

Figure 7. The N-Myc cistrome is altered upon Rb1 loss. A. Venn diagram showing the overlap of N-Myc binding by ChIP-seq from *MYCN+;Rb1*$^{f/f}$ (n=3) and *MYCN+* (n=2) tumors (peak cutoff: q < 0.0001). **B.** Differential transcription factor motif enrichment between N-Myc binding sites in *MYCN+;Rb1*$^{f/f}$ and *MYCN+* tumors. **C.** Heatmaps of N-Myc binding in *MYCN+;Rb1*$^{f/f}$ and *MYCN+* tumors at regions of accessible chromatin associated with neuroendocrine and luminal subpopulations by scATAC-seq in Figure 5C. **D.** N-Myc binding at indicated loci in *MYCN+;Rb1*$^{f/f}$ (n=3) and *MYCN+* (n=2) tumors.

What opportunities for training and professional development has the project provided?

Presentations:

- Prostate Cancer Foundation, Carlsbad, CA.
  Annual Scientific Retreat
- Multi-Institutional Prostate Cancer Program Retreat, Los Angeles, CA
  Annual meeting of institutions with an NCI-funded P50 SPORE grant in prostate cancer research.
- AACR Special Conference: Advances in Prostate Cancer, Denver, CO

Workshops/Training Opportunities:

- Biostatistics Seminar Series (WCM)
  This is a monthly lecture series geared towards clinical investigators, research staff, and students who are interested in gaining insight into fundamental research design and statistical concepts with a focus on practical knowledge.
- Transitioning to Research Independence (WCM/Tri-I)

A set of seminars to help you attain and maintain a successful career in academic research

- Workshops through Applied Bioinformatics Core (WCM/Tri-I)
  Regularly held, intensive 12-hours-long courses open to members of the Tri-Institutional network
- Trainee Affairs Career Symposium and Networking Dinner, SBUR Meeting
  Focused on career development plans and the nuts and bolts of setting up and running a research lab
- AACR Translational Research for Basic Scientists Workshop.
  An innovative 1 week workshop for basic scientists pursuing training in order to transition into translational cancer research
- *Ad hoc* reviewer for Cancer Cell, Molecular Cell, Nature Communications, Cell Reports and Science Translational Medicine, JCI, Nature Medicine, Nature, Clinical Cancer Research, PNAS
  Critically reviewed manuscripts for publication in related fields

Drs Beltran and Rickman are fully committed to furthering the training and professional development of the post-doctoral fellows and students affiliated to this project. This has including presentations at PCF, AACR, Prostate Cancer SPORE Retreats, SBUR meetings. Dr. Nick Brady (postdoctoral fellow in the Rickman lab) received prize for best abstract at the; Prostate Cancer SPORE program Annual Retreat, February 2020. Nick also competed successfully for an American Cancer Society postdoctoral award (awarded Aug 2020). Dr. Richa Singh (Rickman lab) and Dr. Balaji Venkadakrishnan (Beltran lab) received Department of Defense postdoctoral training awards. Balaji Venkadakrishnan also received a National Cancer Center (NCC) Fellowship.

Postdoc fellows also participate in the following:
NIH T32 MTOR Course. 15 lectures, especially designed for MTOR, will be presented by our preceptors jointly with their clinical collaborators to showcase the principles of translational cancer research and team science.

Transitioning to Research Independence seminar series. A seminar series geared towards postdoctoral researchers and fellows who plan to set up their own laboratory and develop their own research program at an academic institution. Trainees will comprehend the faculty application process; understand strategies for funding, mentoring and leadership to effectively run their own research group.

Biostatistics Lecture Series through the Clinical and Translational Science Center. This is a monthly lecture series geared towards clinical investigators, research staff, and students who are interested in gaining insight into fundamental research design and statistical concepts with a focus on practical knowledge.

Broad Institute of MIT and Harvard, Computational Biology Workshops. Fellows in the Beltran particitpate in short courses and workshops online for computational programming.

AACR Translational Research for Basic Scientists Workshop. Drs. Balaji Venkadakrishnan and Martin Bakht postdoctoral fellows in the Beltran lab were selected to in this intensive one week workshop in 2022. The Translational Cancer Research for Basic Scientists Workshop provides basic research scientists with essential training to adapt their research for maximum clinical impact and transition into a new career in translational cancer medicine

How were the results disseminated to communities of interest?

We presented at the Multi-institutional Prostate Cancer Meeting in Ft Lauderdale in February 2022 which is organized and led by the SPORE programs. Dr. Rickman will also present data at AACR Prostate Meeting in March 2023. The following manuscripts are related to this project:

1. Puca, L., et al., **Nat Commun**, 2018. 9(1): p. 2404.

2. Beltran, H., et al., **Clin Cancer Res**, 2018.

3. Beltran et al. **Clinical Cancer Research** (2019)

4. Puca L... Beltran H, **Science Translational Medicine** (2019)

5. Berger, A., Brady, N … Rickman DS, **Journal of Clinical Investigation** (2019)

6. Beltran et al… **Clinical Cancer Research** (2019)

7. Conteduca V. et al…. Beltran H**. European Journal of Cancer** (2019)

8. Beltran et al… **Journal of Clinical Investigation** (2020)

9. Brady, N., et al. …Beltran, H.,..Rickman, DS *Temporal evolution of cellular heterogeneity during the progression to advanced, AR-negative prostate cancer*, **Nature Communications** (2021)

10. Conteduca et al… Beltran, **NPJ Precision Oncology** (2021)

What do you plan to do during the next reporting period to accomplish the goals?

Related to Aim 1, we will continue evaluation of tumors and blood samples from patients across the diseae continuum to better understand the timing of N-myc in driving lineage plasticity and the role and timing of co-occuring genomic aberrations (eg., RB1, TP53) and epigenetic changes (eg., DNA methylation). We have now expanded analyses to include CTCs and cfDNA so that we can evaluate sequential samples non-invasively, which we will continue in the coming uyear.

Related to Aim 2, we will continue our analyses of the N-Myc cistrome and how other transcription factors (e.g. ASCL1 and POU2F3) may function to mediate the driving role of N-Myc on the the molecular program associated with NEPC. For this we will rely on our new GEM described above. We will perform genetic experiments (knock-in/knock-out) of specific cofactors to determine their cooperative role with N-Myc in driving this phenotype.

Related to Aim 3, we continue to develop and test novel EZH2 combination strategies in vitro and in vivo. The studies are ongoing. We hope to generate data to inform future biomarker-driven clinical trials.

4. IMPACT:

What was the impact on the development of the principal discipline(s) of the project?

While *RB1* loss is common in prostate cancer and N-Myc overexpression occurs in a large proportion of NEPC, little is known about the potential synergy between these two events. Here, we are evaluating patient cohorts along the continuum, exploring N-myc expression/amplification and co-occuring genomic and epigenomic data, to determine the timing of N-myc in driving lienage plasticity and impact of other NEPC alterations (eg., RB/TP53 loss, DNA methylation changes). These studies are still ongoing but are leveraging tissue and blood samples from valuable clinically annotated cohorts. There are important biomarker implications when developing the optimal time to target /co-target N-myc and lineage plasticity To study the mechanism behind this association, we have also generated a GEM combining dual *Pten* and *Rb1* loss with N-Myc overexpression. These mice rapidly developed tumors with poorly differentiated histology and were significantly more castration-resistant than control animals.

The degree of differences between the transcriptomes of specific histologies (e.g. adenocarcinoma vs. poorly differentiated/NEPC) based on bulk RNA-seq was not surprising given the dramatic phenotypic differences. However, the striking differences in the N-Myc cistrome in the context of Rb1 loss were intriguing and unexpected, and we hypothesized that cofactors and/or other transcription factors could account for these differences. Interestingly, we observed an enrichment of E2F and MYC targets in poorly differentiated tumor foci compared to adenocarcinoma, suggesting that E2F and N-Myc may have altered or enhanced activity in the transition from adenocarcinoma to a poorly differentiated state. This was also reflected in our ChIP-seq studies where E2F motifs were enriched at N-Myc binding sites that were uniquely found in poorly differentiated tumors. For N-Myc, this is consistent with our previous findings that the N-Myc cistrome can be dynamically regulated [2]. However, in the context of androgen withdrawal, N-Myc binding sites were enriched for Forkhead motifs. Interestingly, the FOXA1 motif was equally enriched in both *MYCN+* and *MYCN+;Rb1*$^{f/f}$ tumors. Instead, the enrichment of an E2F motif at N-Myc binding sites in the context of *Rb1* loss suggests that N-Myc binds at E2F target genes and synergizes to drive a tumorigenic transcriptional state. Further work is needed to determine if E2F transcription factors cooperate with N-Myc and redirects N-Myc binding in the context of *RB1* loss. Downregulated genes were enriched in epigenetic reprogramming and PRC2 targets, as well as epithelial identity, AR signaling and P53 targets. Our previous work demonstrated that N-Myc activates EZH2 transcriptional reprogramming, which plays an important role in driving neuroendocrine prostate cancer [3]. Enrichment of PRC2 target genes and epigenetically marked genes (H3K27me3, associated with repression) suggests a shift in epigenetic reprogramming mediated by PRC2 when cells transition from adenocarcinoma to a poorly differentiated/NEPC phenotype. We also observed downregulation of genes related to epithelial identity, such as those that are downregulated by loss of epithelial adhesion molecule E-cadherin (CDH1). Loss of E-cadherin is thought to promote metastasis through the initiation of EMT and invasiveness [19]. We primarily saw metastatic lesions with poorly differentiated histology in our GEMs and mouse allografts, suggesting that poorly differentiated cells have higher metastatic potential due to activation of EMT pathways. Interestingly, our use of organoid-derived subcutaneous allografts revealed that the development of NEPC-like disease can occur in the context of *Rb1* loss and N-Myc overexpression independently of the prostate microenvironment. Further studies are needed to fully appreciate the role of the tumor microenvironment in shaping early prostate tumorigenesis.

Using RRBS to query changes in DNA methylation across our *in vivo* and *in vitro* models, as well as patient samples, we found that components of the DNA methylation machinery were deregulated in poorly differentiated/NE tumors compared to adenocarcinomas. This corresponded to differential methylation statuses across a number of clinically relevant loci throughout the genome. Based on our methylation data from GEM tumors, we developed a 360 gene methylation signature which successfully segregated clinical CRPC and NEPC samples. It remains to be seen how levels of DNA methylation track with levels of H3K27me3 and chromatin accessibility.

Given the heterogeneity in the developing tumors, single-cell based approaches allowed for a refined characterization of the oncogenic transformation. Single cell RNA-seq studies recapitulated our previous reports of the role of N-Myc and EZH2 cooperating to suppress AR signaling [2,3]. We have also demonstrated that the population of cells expressing known neuroendocrine markers also showed increased expression of a gene expression signature correlated with poor survival in patients [16]. Of particular note, we found an upregulation of a number of neuroendocrine marker genes in cells that were not part of the distinct neuroendocrine cluster and were a large distance away in pseudotime. These data strongly support the notion that cells transition from a luminal-like state towards an NEPC-like state and are not simply an expansion of existing neuroendocrine precursor cells. Moreover, as many of these cells expressed AR but had low levels of AR target genes, it suggests that pharmacologic inhibition of EZH2 may restore androgen signaling and reverse the induced NE transcriptional program. This is particularly relevant as a number of clinical trials using EZH2 inhibitors are currently in progress, including many in prostate cancer (NCT03480646, NCT04179864, NCT03460977). Additionally, both our scRNA-seq and scATAC-seq studies found two distinct neuroendocrine clusters on the basis of transcription and chromatin accessibility. These two clusters differed in their expression of *Ascl1 and Pou2f3* as well as in their enrichment for ASCL

and POU/OCT transcription factor family binding motifs. Recent work in small cell lung cancer (SCLC) has found Notch activation in c-Myc-driven tumors can promote a switch between ASCL1-positive, NEUROD1-positive, and YAP1-positive states [20]. Our previous studies have shown that, while c-Myc and N-Myc share a number of common target genes, the N-Myc cistrome in prostate cells encompasses a larger and more diverse set of transcriptional targets [2]. We did find enrichment of NeuroD1 motifs in the scATAC-seq data from one of the neuroendocrine subpopulations. It is possible that changes to accessible motifs mark populations that are undergoing a transition between states. Additional work is needed to understand how these two subpopulations are regulated and if there are different lineage outcomes for a cell depending on which of the populations served as cluster of origin.

Altogether, our studies have identified a population of cells which downregulate AR signaling and undergo a lineage transformation to a neuroendocrine-like phenotype following N-Myc over-expression and *Pten/Rb1* co-loss. This lineage change was accompanied by changes in chromatin accessibility and N-Myc binding at a number of clinically relevant genes. Finally, we identified a methylation signature which may inform future clinical trials using EZH2 inhibitors as to which patients are most likely to benefit from EZH2 inhibition and as a biomarker to identify patients who show a beneficial response. We are expanding on this to further characterize biomarkers of response to EZH2 inhbition in GEMM and patient-derived organoids/PDX modelds of NEPC. We are alos developing rationale combinations approaches to sensitize to EZH2 inhibitor therapy. We hope to eventually translate these findings to the clinic.

Overall these studies are starting to shed light on the molecular mechanisms by which N-Myc overexpression and *Rb1* loss synergize to drive the development of neuroendocrine prostate cancer and have provided new avenues of exploration towards identifying and validating new therapeutic targets.

References

1 Beltran, H. *et al.* Molecular characterization of neuroendocrine prostate cancer and identification of new drug targets. *Cancer Discov* **1**, 487-495, doi:10.1158/2159-8290.CD-11-0130 (2011).

2 Berger, A. *et al.* N-Myc-mediated epigenetic reprogramming drives lineage plasticity in advanced prostate cancer. *J Clin Invest* **130**, 3924-3940, doi:10.1172/JCI127961 (2019).

3 Dardenne, E. *et al.* N-Myc Induces an EZH2-Mediated Transcriptional Program Driving Neuroendocrine Prostate Cancer. *Cancer Cell* **30**, 563-577, doi:10.1016/j.ccell.2016.09.005 (2016).

4 Lee, J. K. *et al.* N-Myc Drives Neuroendocrine Prostate Cancer Initiated from Human Prostate Epithelial Cells. *Cancer Cell* **29**, 536-547, doi:10.1016/j.ccell.2016.03.001 (2016).

5 Ku, S. Y. *et al.* Rb1 and Trp53 cooperate to suppress prostate cancer lineage plasticity, metastasis, and antiandrogen resistance. *Science* **355**, 78-83, doi:10.1126/science.aah4199 (2017).

6 Mu, P. *et al.* SOX2 promotes lineage plasticity and antiandrogen resistance in TP53- and RB1-deficient prostate cancer. *Science* **355**, 84-88, doi:10.1126/science.aah4307 (2017).

7 Balanis, N. G. *et al.* Pan-cancer Convergence to a Small-Cell Neuroendocrine Phenotype that Shares Susceptibilities with Hematological Malignancies. *Cancer Cell* **36**, 17-34 e17, doi:10.1016/j.ccell.2019.06.005 (2019).

8 Rosenbaum, J. N. *et al.* INSM1: A Novel Immunohistochemical and Molecular Marker for Neuroendocrine and Neuroepithelial Neoplasms. *American journal of clinical pathology* **144**, 579-591, doi:10.1309/AJCPGZWXXBSNL4VD (2015).

9 Agoff, S. N. *et al.* Thyroid transcription factor-1 is expressed in extrapulmonary small cell carcinomas but not in other extrapulmonary neuroendocrine tumors. *Mod Pathol* **13**, 238-242 (2000).

10 Zhou, Z. *et al.* Synergy of p53 and Rb deficiency in a conditional mouse model for metastatic prostate cancer. *Cancer Res* **66**, 7889-7898, doi:66/16/7889 [pii]
10.1158/0008-5472.CAN-06-0486 (2006).

11 Dubchak, I. *et al.* Active conservation of noncoding sequences revealed by three-way species comparisons. *Genome Res* **10**, 1304-1306, doi:10.1101/gr.142200 (2000).

12 Frazer, K. A., Pachter, L., Poliakov, A., Rubin, E. M. & Dubchak, I. VISTA: computational tools for comparative genomics. *Nucleic Acids Res* **32**, W273-279, doi:10.1093/nar/gkh458 (2004).
13 Cerami, E. *et al.* The cBio cancer genomics portal: an open platform for exploring multidimensional cancer genomics data. *Cancer Discov* **2**, 401-404, doi:10.1158/2159-8290.CD-12-0095 (2012).
14 Gao, J. *et al.* Integrative analysis of complex cancer genomics and clinical profiles using the cBioPortal. *Sci Signal* **6**, pl1, doi:10.1126/scisignal.2004088 (2013).
15 Beltran, H. *et al.* Divergent clonal evolution of castration-resistant neuroendocrine prostate cancer. *Nat Med* **22**, 298-305, doi:10.1038/nm.4045 (2016).
16 Smith, B. A. *et al.* A Human Adult Stem Cell Signature Marks Aggressive Variants across Epithelial Cancers. *Cell Rep* **24**, 3353-3366 e3355, doi:10.1016/j.celrep.2018.08.062 (2018).
17 Trapnell, C. *et al.* The dynamics and regulators of cell fate decisions are revealed by pseudotemporal ordering of single cells. *Nat Biotechnol* **32**, 381-386, doi:10.1038/nbt.2859 (2014).
18 Korenjak, M., Anderssen, E., Ramaswamy, S., Whetstine, J. R. & Dyson, N. J. RBF binding to both canonical E2F targets and noncanonical targets depends on functional dE2F/dDP complexes. *Mol Cell Biol* **32**, 4375-4387, doi:10.1128/MCB.00536-12 (2012).
19 Onder, T. T. *et al.* Loss of E-cadherin promotes metastasis via multiple downstream transcriptional pathways. *Cancer Res* **68**, 3645-3654, doi:10.1158/0008-5472.CAN-07-2938 (2008).
20 Ireland, A. S. *et al.* MYC Drives Temporal Evolution of Small Cell Lung Cancer Subtypes by Reprogramming Neuroendocrine Fate. *Cancer Cell*, doi:10.1016/j.ccell.2020.05.001 (2020).

What was the impact on other disciplines?
Results from this study may provide insights in other cancer types that develop lineage plasticity as a resistance mechanism to targeted therapies (eg., EGFR mutated lung adenocarcinomas that transform to small cell carcinoma), as there are shared molecular features and potentially shared therapeutic implications.

What was the impact on technology transfer?
Nothing to Report

What was the impact on society beyond science and technology?
Nothing to Report

5. CHANGES/PROBLEMS:

Changes in approach and reasons for change

No changes/problems to report

Actual or anticipated problems or delays and actions or plans to resolve them
Nothing to report

Changes that had a significant impact on expenditures
Nothing to report

Significant changes in use or care of human subjects, vertebrate animals, biohazards, and/or select agents
Nothing to report

Significant changes in use or care of human subjects

Nothing to report

Significant changes in use or care of vertebrate animals.
Nothing to report

Significant changes in use of biohazards and/or select agents
Nothing to report

6. PRODUCTS:

- **Publications, conference papers, and presentations**

  Journal publications.

1. Puca, L., et al., **Nat Commun**, 2018. 9(1): p. 2404., yes
2. Beltran, H., et al., **Clin Cancer Res**, 2018., yes
3. Beltran et al. **Clinical Cancer Research** (2019), yes
4. Puca L... Beltran H, **Science Translational Medicine** (2019), to a small degree
5. Berger, A., Brady, N … Rickman DS, **Journal of Clinical Investigation** (2019), yes
6. Beltran et al… **Clinical Cancer Research** (2019) , yes
7. Conteduca V. et al…. Beltran H**. European Journal of Cancer** (2019), yes
8. Beltran et al… **Journal of Clinical Investigation** (2020), yes
9. Brady, N., et al. …Beltran, H.,..Rickman, DS *Temporal evolution of cellular heterogeneity during the progression to advanced,* **Nat Commun**, 2018, yes

  Books or other non-periodical, one-time publications.
  Nothing to report

  Other publications, conference papers, and presentations.

  We presented this data at the AACR – Prostate Cancer December 2017 and will present at the next AACR Prostate in March 2023, Denver CO; Prostate Cancer SPORE programs Annual Retreat, February 2018, 2019, 2020, 2022; AACR April 2018, 2019, 2023; Society of Basic Urologic Research, 2018, 2019, 2023.

- **Website(s) or other Internet site(s)**
  Nothing to report

- **Technologies or techniques**
  Nothing to report

- **Inventions, patent applications, and/or licenses**
  Nothing to report

- **Other Products**
  Nothing to report

7. PARTICIPANTS & OTHER COLLABORATING ORGANIZATIONS

What individuals have worked on the project?

Name:	Himisha Beltran, MD
Project Role:	PI
Researcher Identifier (e.g. ORCID ID):	0000-0003-3259-2226
Nearest person month worked:	3
Contribution to Project:	Work on Aim 1,2,3
Funding Support:	

Name:	Sheng-Yu Ku
Project Role:	Post-Doctoral Associate
Researcher Identifier (e.g. ORCID ID):	
Nearest person month worked:	1
Contribution to Project:	Aims 1, 3
Funding Support:	

Name:	Kei Mizuno
Project Role:	Post-Doctoral Associate
Researcher Identifier (e.g. ORCID ID):	
Nearest person month worked:	12
Contribution to Project:	Aims 1, 3
Funding Support:	Japan Society for the Promotion of Science Oversees W81XWH-17-1-0653

Name:	Varadha Balaji Venkadakrishnan
Project Role:	Post-Doctoral Associate
Researcher Identifier (e.g. ORCID ID):	
Nearest person month worked:	3
Contribution to Project:	Work on Aim 1,3
Funding Support:	

Has there been a change in the active other support of the PD/PI(s) or senior/key personnel since the last reporting period?

Beltran, Himisha

PREVIOUS:

ENDED
DFCI SRA-21-0376 05/01/21 – 12/31/22
Bristol Myers Squibb
Restoration of Antigen Presentation, Innate Immune Signaling, and Cellular Differentiation by Epigenetic Inhibitors in Small Cell Lung and Neuroendocrine Prostate Cancer
Specific Aims: 1) Identify the relative impact of LSD1 inhibitors or EZH2 inhibitors treatment on derepression

of MHC class I, markers of innate immune signaling, and loss of neuroendocrine differentiation across multiple preclinical models of small cell lung cancer (SCLC) and neuroendocrine prostate cancer; 2) Determine whether LSD1 and EZH2 inhibition synergize to derepress MHC class I, innate immune signaling, and cause loss of neuroendocrine differentiation.
Role: Principal Investigator
POC: Protocol Manager: Donette Quamina-Edghill; donette.quaminaedghill@bms.com; 609-302-4189

ENDED
W81XWH-19-1-0403 (Barbieri) 09/23/19 – 09/29/22
Department of Defense
Defining the Potential of Early Molecular Subtypes of Prostate Cancer to Progress to AR-Indifferent Disease
Specific Aims: 1) Define genomic subclasses of early PCa that are susceptible or resistant to conversion to NEPC; 2) Determine if SPOP mutations prevent N-Myc driven conversion to NEPC using unique preclinical platforms.
Role: Co-Investigator
POC: Grants Officer: Joshua D. McKean; joshua.d.mckean3.civ@mail.mil

ENDED
W81XWH-18-PCRP-IDA (Giannakakou) 08/15/19 – 08/14/22
Department of Defense
Transferrin Receptor Identifies a Comprehensive Pool of Circulating Tumor Cells with Unique Molecular Features from Metastatic Prostate Cancer Patients
Specific Aims: Perform molecular profiling of tumors and analysis and help integrate results with patient data and other platforms in the study.
Role: Co-Investigator
POC: Grants Officer: Joshua D. McKean; joshua.d.mckean3.civ@mail.mil

ENDED
P50CA211024 (Loda) 08/01/17 – 07/31/22
National Cancer Institute
Weill Cornell Medicine (WCM) SPORE in Prostate Cancer
Project 2: Targeting N-MYC and EZH2-Driven Castrate Resistant Prostate Cancer
Specific Aims: The goal of this project is to develop more effective targeting strategies for a biomarker-selected subgroup of late stage CRPC driven by N-Myc and less dependent on the AR.
Roles: Co-Principal Investigator; Project 2 Co-Leader
POC: Program Director, Translational Research Program: Julia T. Arnold; jarnold@mail.nih.gov;

CURRENT:

NEW
22CHAL08 01/06/23 – 01/05/25 0.60 CM
Prostate Cancer Foundation
Mechanisms of Response and Resistance to DLL3-Targeted T Cell Engager Therapy
Specific Aims: 1) Improve patient selection for a DLL3-targeted T cell engager therapy; 2) Investigate the therapeutic potential of DLL3-Targeted T cell engagers and resistance mechanisms.
Role: Principal Investigator
POC: Program Administration Manager: Audrey Gardener; agardner@pcf.org;

NEW
22003-01 01/01/23 – 06/30/24 0.30
CM DFCI DDTRP
Dissecting Tumor Heterogeneity in Lethal Castration Resistant and Neuroendocrine Prostate Cancer
Specific Aims: 1) Understand the interplay between epigenetics and metabolism of liver versus non-liver metastases in CRPC and NEPC; 2) Map tumor transcriptomic and metabolomic profiles as prostate cancer evolves from a mixed adeno-NE tumor to NEPC and test response of PSMA-positive NEPC tumors to LuPSMA-617
Role: Principal Investigator
POC: DDTRP Program Administrator: Sylvia Lin; Sylvia_Lin@dfci.harvard.edu;

NEW
TellDx CTC System 12/01/22 – 11/30/23 0.60 CM
National Foundation for Cancer Research
Characterization of circulating tumor cells from patients with genitourinary malignancies
Specific Aims: 1) To perform molecular subtyping of kidney cancer using CTCs; 2) To detect the NEPC features using CTCs.
Role: Principal Investigator
POC: Director of Institute Relations: Hali Hartmann; hhartmann@nfcr.org;

NEW
R01 CA270539 (Dehm) 12/01/22 – 11/30/27 0.49
CM National Institutes of Health
Targeting early events in prostate cancer lineage plasticity
Specific Aims: There will be 10-20 drugs nominated by Dr. Dehm's lab in Years 1-3 for testing by Dr. Beltran and her team in Years 3-5. Readouts in the PDO assays will be growth/viability and for certain efficacious drugs some follow-up IF/IHC and RT-PCR for lineage plasticity markers where warranted.
Role: Co-Principal Investigator
POC: Program Official: Tapan K. Bera; berat@mail.nih.gov;

NEW
W81XWH-21-PCRP-IDA (Aytes) 10/01/22 – 09/30/25 0.30 CM
Department of Defense
Dissecting the role of cancer cell chromatin remodeling on the landscape of tumor immune microenvironment
Specific Aims: 1) Dr. Beltran and her laboratory will contribute to the project by performing preclinical studies using patient derived organoids of NEPC/CRPC and prostate cancer biopsies from metastatic prostate cancer patients for single cell sequencing and other molecular analyses; 2) Dr. Beltran's lab will also carry on a HT drug screen will cells shipped from Dr. Aytes's lab to Dr. Beltran's using the HT-screening platforms at DFCI; 3) Dr. Beltran and her lab will contribute to data analysis and integration
Role: Co-Investigator
POC: Grants Officer: Joshua D. McKean; joshua.d.mckean.civ@mail.mil

NEW
P50 CA092629 (Scher) 09/01/22 – 08/31/27 0.20 CM
National Institutes of Health
Project 3: Therapeutic Targeting of Lineage Plasticity in Castration-Resistant Prostate Cancer
Specific Aims: 1) Dr. Beltran will help oversee ctDNA and tissue methylation aspects of this project and work closely with members of the team to integrate efforts, analyze results, and prioritize data; 2) Her lab will also perform drug testing using patient derived organoids.
Role: Co-Investigator

POC: Program Coordinator, Translational Research Program: Mehvish Khan; khanm11@mail.nih.gov

NEW
DFCI SRA-DS-7300 06/01/22 – 05/31/24 0.30 CM
Daiichi Sankyo, Inc.
Targeting B7-H3 in neuroendocrine prostate cancer
Specific Aims: 1) Determine the anti-tumor activity of DS-7300a, decitabine, and the combination in CRPC/NEPC in in-vitro and in-vivo models; 2) Elucidate the expression and clinical associations of B7-H3 in our patient cohorts and preclinical models of CRPC/NEPC
Role: Principal Investigator
POC: Associate Director, US Medical Affairs, Research and Strategy – Oncology: Diederik van Bodegom; dvanbodegom@dsi.com

NEW
DFCI SRA-22-1663 03/01/22 – 02/29/23 0.60
CM Circle Pharma, Inc.
Targeting Cyclin-CDK2 complex in RB dysregulated advanced prostate cancer
Specific Aims: To define the therapeutic activity of targeting Cyclin-CDK complex
Role: Principal Investigator
POC: Vice President, Translational Medicine: Evelyn Wang; evelyn.wang@circlepharma.com;

What other organizations were involved as partners?
Nothing to report

8. SPECIAL REPORTING REQUIREMENTS
Nothing to report

9. APPENDICES
Nothing to report